1 **Mycobacteria form viable cell wall-deficient cells that are undetectable by**

2 **conventional diagnostics**

3 Noortje Dannenberg[1], Victor J. Carrion Bravo[1, 2, 3], Tom Weijers[1], Herman P.

4 Spaink[1], Tom H. M. Ottenhoff[4], Ariane Briegel[1, 5] & Dennis Claessen[1*]

5

6 [1] Institute of Biology, Leiden University, Sylviusweg 72, 2333 BE Leiden, The

7 Netherlands.

8 [2] Departamento de Microbiología, Instituto de Hortofruticultura Subtropical y

9 Mediterránea 'La Mayora', Universidad de Málaga-Consejo Superior de

10 Investigaciones Científicas (IHSM-UMA-CSIC), Universidad de Málaga, Málaga,

11 Spain

12 [3] Department of Microbial Ecology, Netherlands Institute of Ecology (NIOO-KNAW),

13 Wageningen, the Netherlands

14 [4] Infectious Diseases, Leiden University Medical Center, Albinusdreef 2, 2333 ZA

15 Leiden, The Netherlands

16 [5] Netherlands Centre for Electron Nanoscopy (NeCEN), Leiden University,

17 Einsteinweg 55, 2333 CC Leiden, The Netherlands

18

19 *Correspondence: d.claessen@biology.leidenuniv.nl

20

21 **KEYWORDS**

22 **Mycobacteria, cell wall-deficiency, viability, antibiotics, osmolality, diagnostics**

ABSTRACT

The cell wall is a unifying trait in bacteria and provides protection against environmental insults. Therefore, the wall is considered essential for most bacteria. Despite this critical role, many bacteria can transiently shed their cell wall and recent observations suggest a link of such wall-deficient cells to chronic infections. Whether shedding the cell wall also occurs in mycobacteria has not been established unambiguously. Here we provide compelling evidence that a wide range of mycobacterial species, including clinical and non-clinical isolates, form viable cell wall-deficient cells in response to environmental stressors. Using cryo-transmission electron micrography we show that the complex multi-layered wall is largely lost in such cells. Notably, we show that their formation in *Mycobacterium marinum* and BCG vaccine strains of *Mycobacterium bovis* is stimulated by exposure to cell wall-targeting antibiotics. Given that these wall-deficient mycobacteria are undetectable using conventional diagnostic methods, such cells have likely been overlooked in clinical settings. Altogether, these results indicate that mycobacteria can readily switch between a walled and wall-deficient lifestyle, which provides a plausible explanation for enabling persistence of infections caused by members of this genus.

INTRODUCTION

Mycobacteria are the causative agents of some of the most serious human infectious diseases, including tuberculosis (TB), leprosy and a range of other infections (WHO, 2020; WHO, 2021). Upon transmission, these pathogens cause progressive infections that need to be treated with elaborate antibiotic regimes. However, such treatments may stimulate persistence in the host and promote the development of antibiotic resistance (Simmons *et al.,* 2018, Johansen *et al.,* 2020, Saxena *et al.*, 2021). Tackling persistence is challenging because these cells are difficult to cultivate and phenotypically heterogeneous. Therefore, many fundamental questions regarding their physiological state and mechanism of survival remain unanswered (Barry *et al*., 2009; Dhar and McKinney, 2007; Manina *et al*., 2014).

Despite being viewed with scepticism, some studies have indicated that mycobacterial persister cells could be cell wall-deficient (CWD), although these studies have been difficult to replicate due to extreme long incubation times of the *in vitro* persistence models (Shleeva *et al*., 2011; Velayati *et al*., 2016). The cell wall is a unifying trait in the bacterial domain and considered essential for most bacteria (Vollmer *et al*., 2008). As such, the enzymes involved in cell wall synthesis are among the prime targets of effective antibiotics, which typically act by preventing normal cell wall assembly and thereby causing cell death. Considering the importance of the cell wall, it is surprising that under specific stressful conditions a range of bacteria can transiently escape from their enclosing cell wall to adopt a viable but CWD lifestyle (Allan *et al*., 2009; Claessen and van Wezel, 2014; Errington, 2013, 2017; Errington *et al*., 2016; Kawai *et al*., 2015; Klieneberger, 1935; Mercier *et al*., 2014; Ramijan *et al*., 2018; Claessen and Errington, 2019, Lazenby *et al.,* 2022). These cells are competent with regard to DNA uptake (Woo *et al.,* 2003, Kapteijn *et al.,* 2022) and can revert to their walled state when the stressful conditions have diminished. Furthermore, these cells can oftentimes proliferate without their cell wall, as so-called "L-forms", under specific growth conditions or through the acquirement of beneficial mutations. Such mutations are known to reduce susceptibility to reactive oxygen species (ROS) and to increase membrane fluidity. Importantly, the loss of the cell wall provides a mechanism via which bacteria are protected from cell wall-targeting antibiotics (Kawai *et al*., 2018). Besides, as the most important antigens of bacteria

72   are located on the cell surface, loss of the cell wall could potentially facilitate immune

73   evasion and contribute further to persistence in the host (Källenius *et al*., 2016).

74   Recent observations suggest a link between cell wall-deficiency and chronic

75   infections, based on the isolation of *Escherichia coli* CWD cells from patients suffering

76   from recurrent urinary tract infections (Mickiewicz *et al*., 2019). This raises the question

77   whether CWD may also play a role in other infectious diseases, such as tuberculosis.

78   In this study, we show that multiple mycobacterial species can naturally form viable

79   CWD cells in response to environmental stressors. Confocal microscopy and cryo-

80   transmission electron microscopy confirmed that these cells contain DNA but lack

81   major cell wall structures. Importantly, in *Mycolicibacterium smegmatis,* mycobacterial

82   endophyte isolates (Carrion *et al*., 2019), clinical isolates of the *Mycobacterium avium*

83   complex, *Mycobacterium marinum* strains and *Mycobacterium bovis* BCG vaccine

84   strains formation of these cells is stimulated by the presence of cell wall-targeting

85   agents, including isoniazid, D-cycloserine and vancomycin, of which the former two

86   are used clinically to treat infections. Furthermore, we show that conventional

87   diagnostics fail to detect CWD cells, suggesting that such cells may have been over-

88   looked in clinical diagnostic settings. Altogether, our work provides important insights

89   in morphological and phenotypic plasticity in mycobacteria, which in the future may be

90   exploited to target these devastating pathogens.

91

RESULTS

Mycobacteria produce wall-deficient cells under hyperosmotic stress conditions

95   To investigate the ability of Mycobacteria to generate CWD cells, we grew the fast-

96   growing model organism *Mycolicibacterium smegmatis* mc^{2}155 in media containing

97   high levels of osmolytes, which was previously used for the formation of CWD cells in

98   other actinobacteria (Ramijan *et al.,* 2018). Interestingly, growth of *M. smegmatis* on

99   solid L-Phase Media Agar (LPMA) resulted in a change in colony morphology.

100   Whereas on standard Middlebrook 7H10 medium colonies appeared rough and white,

101   those on LPMA were small and transparent (Fig. 1A). Further investigation by light

102   microscopy revealed spherical, vesicular structures between the elongated

103   mycobacterial cells on LPMA, which were not found when using 7H10 medium. Similar

104   vesicles were also identified when the strain was grown in liquid L-Phase Broth (LPB)

105   and these vesicles contained nucleic acids as revealed by labelling with SYTO 9 (Fig.

106   1B). By using a constitutively expressing mCherry strain, these vesicles were found to

107   contain fluorescent cytosol (Fig. 1C, S1D), perhaps suggesting that they are

108   metabolically active cells. Indeed, these cells increased in size over time, from an

109   average of 1.03 ± 0.54 μm (n = 561) to 2.15 ± 0.97 μm (n = 684) after 1 day and 10

110   days, respectively. Some cells even reached a size of more than 5 μm, coinciding with

111   an increased complexity of the cellular content (Fig. 1D, S1).

112   To gain insight into the origin of the spherical cells in the context of the rod-

113   shaped cells, we performed live imaging (Fig. 1E, Video S1). These experiments

114   revealed that these cells were extruded from the tips of the polar growing cells. In

115   addition, their abundance positively correlated with an increased sucrose

116   concentration in the medium (Fig. 1F, S1E, S2), while inversely correlating to growth

117   of the strain (Fig. 1G, S1F). Importantly, formation of these cells is not restricted to *M.*

118   *smegmatis* mc²155. We also noticed that the parental strain isolated from human

119   samples, *Mycolicibacterium smegmatis* ATCC607, forms such spherical cells in the

120   presence of high sucrose concentrations (Fig. 1H). Likewise, such cells were found in

121   clinical, veterinary and lab strains of *Mycobacterium avium* Complex (MAC), as well

122   as endophytic *Mycobacterium* isolates from sugar beet (Fig. 1H, S3A). Interestingly,

123   the veterinary specimen *Mycobacterium avium* subsp. *Hominissuis* 20-935 /2, isolated

124   from pig liver, produced an excess amount of membrane structures, but the majority

125   did not contain nucleic acids (Fig. S3B).

126   To characterize the spherical cells of *M. smegmatis* in more detail we

127   successfully enriched them through filtration and concentration steps (Fig. S4) and

128   analysed them in their native state. Cryo-transmission electron micrography (TEM)

129   revealed that these cells lack major mycobacterial cell wall components, similarly to

130   protoplasts, in which the cell wall is artificially removed through lysozyme treatment

131   (Fig. 2A, S5). Comparable to protoplasts, the CWD cells are enveloped by the lipid

132   bilayer, which is around 10 nm as seen in the grey value density plot, compared to the

133   45 nm cell envelope of walled cells (Fig. 2B, 2C). In some CWD cells, patches of cell

134   wall material are evident exterior to the cell membrane (Fig. S5D). The diameter of

135   these CWD cells range from 450 – 830 nm, which is similar to protoplasts that are

136   550-1200 nm in size (Fig. 2D). However, these CWD cells are considerably larger than

137   extracellular vesicles, which typically range from 60 – 300 nm (Prados-Rosales *et al.*,

138   2011; 2014; Gupta and Rodrigues, 2018). Furthermore, unlike extracellular vesicles,

139   the content of CWD cells is dark-phased, suggesting dense packaging of macro-

140   molecules. Altogether, these results demonstrate that formation of CWD cells in

141   mycobacteria is a widespread mycobacterial response to hyperosmotic stress

142   conditions.

Mycobacterial wall-deficient cells are viable

144   To analyse if the CWD cells are viable and able to revert to their walled state, we

145   attempted to separate them from walled cells using Fluorescent Activated Cell Sorting

146   (FACS). However, the sensitive nature of the CWD cells complicated cell sorting, as

147   these structures do not withstand the lack of osmo-protectants in the sheet fluid (Data

148   not shown). Therefore, we indirectly tested their viability by removal of the CWD cells

149   through the addition of the non-ionic detergent Triton X-100 (TX-100), a routinely used

150   agent to solubilize membranes (Mattei *et al.* 2017). This treatment results in the

151   formation of pores in the lipid bilayer membrane, causing explosive lysis, while cell-

152   wall containing cells are protected. If the CWD cells are indeed viable, then treating

153   such cells with detergent should result in a measurable drop of colony forming units

154   (CFUs).

155   In accordance with this hypothesis, exposure to TX-100 removed all mCherry

156   labelled CWD cells, while walled cells appeared unaffected (Fig. 3A). Real-time

157   imaging indeed revealed the removal of the fluorescent CWD cells over time (Fig. 3B,

158   Video S2), which was further substantiated by flow cytometric analysis (Fig. 3C, CWD

159   cells: Q3; Pearson Chi-Square test, df = 2; χ^2 =25.15, *p*-value = 3.45e^{-06}; Table S3).

160   Importantly, exposure to TX-100 reduced the formation of colony forming units 60-fold

161   (Paired student t-test, tails 2: *p*-value= 0.012; Table S4), similarly to treatment of

162   protoplasts with this detergent. By contrast, no decline in viability was observed when

163   walled cells were exposed to TX-100. Taken together, these data demonstrate that a

164   substantial fraction of CWD cells contributes to bacterial viability and replication

165   competence as determined by CFU counts.

Antibiotics induce formation of CWD cells in lower sucrose media

167   Cell wall-targeting antibiotics are a mainstay in treatment strategies of mycobacterial

168   infections. To analyse the effect of such antibiotics on formation of CWD cells, we

169   treated the cell cultures with the mycolic acid-targeting compound isoniazid (INH) and

6

170   the peptidoglycan targeting compounds D-cycloserine (DC) and vancomycin (Van).

171   Interestingly, exposure to these three antibiotics stimulated the formation of CWD cells

172   in *M. smegmatis* mc^{2}155 (Fig. 4A). Notably, in the presence of these antibiotics CWD

173   cells became even evident in media with lower levels of sucrose (Fig. 4A, 4B, S7, S8).

174   However, we never detected CWD cells in the standard mycobacterial cultivation

175   media Middlebrook 7H9 or in modified LPB medium without additional sucrose (Fig.

176   S7C). Importantly, investigating other mycobacterial strains under these conditions

177   also revealed the presence of CWD cells, including the vaccine strains *Mycobacterium*

178   *bovis* BCG Pasteur and BCG Russia, as well as *Mycobacterium marinum* M (Fig. 4C,

179   4D, S9). As shown in the phylogenetic tree (Fig. 4E), this indicates a widespread

180   mycobacterial propensity to be able to form CWD cells in the presence of elevated

181   concentrations of cell wall-targeting antibiotics.

182   **Mycobacterial wall-deficient cells are not detected by conventional TB**
183   **diagnostics**

184   Our experiments show that several mycobacteria can form wall-deficient cells under

185   hyperosmotic conditions and that their formation is stimulated by antibiotics. Although

186   CWD cells have been reported in mycobacteria previously, the poor reproducibility of

187   such studies has limited further investigations relating to their clinical relevance. Given

188   that we were reproducibly able to generate and detect CWD cells in a range of

189   mycobacteria, we set out to test whether current cultivation techniques and

190   conventional diagnostics are appropriate to detect CWD cells. Noteworthy,

191   Middlebrook medium (MB7H9), which is the standard cultivation medium for

192   mycobacteria, does not sustain wall-deficient cells (Fig. 5A). However, in line with the

193   previously used LPB medium, the addition of sucrose was sufficient to sustain such

194   wall-deficient cells at a minimum sucrose concentration of 0.2 M (Fig. S10A). To

195   determine the Minimal Osmolar Protection (MOP), the minimal osmolality needed to

196   overcome turgor pressured exploding lysis through osmosis, the osmolality of these

197   conditions was measured (Fig. S9B; Table S7). Interestingly, standard MB7H9 has an

198   osmolality of 144 ± 1 mOsm·kg^{-1}, which is below the minimum of 348 ± 1.2 mOsm·kg^{-1}

199   that is needed to sustain wall-deficient cells (Fig. 5B).

200   These results emphasize the necessity of increasing the osmolality in standard

201   mycobacterial cultivation media to detect cell wall-deficient cells, which should also be

202   considered when visualising cells using common microscopy approaches (Fig. 5C,

203   S9C). For instance, typically used fixation methods appear too harsh for CWD cells,

204   as revealed in samples treated with conventional Acid-Fast Bacterial (AFB) staining

205   methods (Fig. 5D). Notably, we show that the standard Ziehl-Neelsen hot staining

206   method, which incorporates carbol fuchsin in the cytoplasm by heat application, led to

207   destruction of all CWD cells. More specifically, samples containing mixtures of walled

208   and CWD cells revealed abundant background staining but no CWD cells were found.

209   To test whether the boiling steps in the staining procedure affect the preservation of

210   CWD cells, we also applied the cold Kinyoun stain (Kinyoun 1915). This staining

211   appeared to preserve the morphology of CWD cells, including their fluorescence (Fig.

212   5D ROI). However, these cells did not stain red as AFB-positive bacteria as would be

213   expected from mycobacteria. In summary, our experiments reveal that mycobacterial

214   CWD cells are not sustained on routinely used media and remain undetectable by

215   conventional diagnostics (Fig. 5E).

216

DISCUSSION

218   Conventional diagnostics continue to play a pivotal role in clinical settings in terms of

219   detection and identification of pathogenic mycobacteria. In this study, we show that a

220   wide range of mycobacteria undergo morphological transitions to form viable CWD

221   cells in response to hyperosmotic stress and cell wall-targeting antibiotics. Contrary to

222   mycobacterial extracellular vesicles (Prados-Rosales *et al*., 2011; 2014; Gupta &

223   Rodrigues 2018), these CWD cells are larger in size, metabolically active and

224   replication competent. Importantly, the conventional Middlebrook medium, which is

225   used in mycobacterial growth indicator tubes (MGIT) and antibiotic susceptibility

226   testing (Pfyffer *et al*., 1997), is not suitable to sustain mycobacterial CWD cells.

227   Furthermore, traditional Acid-Fast Bacterial staining methods, such as Ziehl-Neelsen,

228   also fail to detect mycobacterial CWD cells. This demonstrates that wall-deficient

229   mycobacteria will not be detected using these classical approaches. Whole-genome

230   sequencing (WGA) has recently been implemented in the diagnostics field,

231   revolutionizing TB detection (Pankhurst *et al.,* 2016). While not experimentally tested

232   here, the procedure of pre-processing the samples includes human cell lysis using

233   osmotic shock (Votintseva *et al.,* 2017), which almost certainly would also destroy

234   CWD cells. Taken together, given that conventional diagnostics are inappropriate to

235   detect CWD cells, they may have been overlooked in clinical settings.

236   The observed shedding of the cell wall appears to be a general mycobacterial
237   stress response, which is stimulated by the presence of antibiotics interfering with
238   peptidoglycan and mycolic acid synthesis. The antibiotics used here included D-
239   cycloserine and isoniazid, respectively, which are typically used in the treatment of
240   (multi-drug resistant) *Mycobacterium tuberculosis* infections (Banerjee *et al.,* 1994;
241   Hwang *et al.,* 2016). Since the closely related vaccine strain *M. bovis* BCG Russia
242   (Borsch *et al.*, 2007) was also shown to form CWD cells in response to these
243   antibiotics, it raises the question if wall-deficiency plays a role in pathogenesis and
244   persistence of *M. tuberculosis.* The formation of such cells may have further
245   contributed to the emergence of multi-, extensively-, and totally drug-resistant
246   (MDR/XDR/TDR) TB strains (Levin-Reisman *et al.*, 2017), given that such wall-
247   deficient cells are more competent for DNA uptake (Kapteijn *et al.,* 2022). The
248   involvement of CWD cells in persistent infections could also explain the necessity of
249   synergistical administration of cell wall-targeting antibiotics with agents that target
250   other essential cellular processes, such as rifampicin (WHO, 2020).

251   Although the association of cell wall-deficiency in a wide range of infectious
252   diseases has been suggested repeatedly, their potential role in chronic or in
253   reoccurring infections remains controversial (Domínguez-Cuevas *et al.*, 2012). More
254   specifically, a CWD state of mycobacteria within the host has been proposed
255   numerous times in clinical *in vivo* and *in vitro* studies (Markova, 2012; Mattman, 1970;
256   Ratnam & Chandrasekhar 1976; Slavchev *et al.*, 2016). However, these studies often
257   lack accurate characterization and therefore remain largely inconclusive (Almenoff *et
258   al.*, 1996; Allan 2009). Therefore, cell wall-deficiency has been traditionally neglected
259   within the mycobacterial field due to difficulties in reproducing and verifying results. In
260   our work, we gained novel insights into the osmotic requirements of these
261   mycobacterial CWD cells, providing reproducible protocols to generate and study this
262   extreme form of morphological plasticity in mycobacteria. Taken together, it would be
263   worthwhile to reinvestigate this phenomenon in terms of treatment persistence to
264   determine its role in mycobacterial pathogenesis and antibiotic resistance.

265   Mycobacteria, like other actinobacterial relatives, incorporate newly
266   synthesized cell wall material at the cellular tips, resulting in apical elongation, via a
267   process known as polar growth (Howell and Brown, 2016). Disrupting the process of
268   mycobacterial cell wall synthesis results in the extrusion of CWD cells at the polar tips.

9

269   This is in line with recent observations in filamentous actinobacteria, in which
270   hyperosmotic stress exposure results in apical extrusion of wall-deficient cells
271   (Ramijan *et al.,* 2018). Since the formation of CWD cells is observed across the
272   mycobacterial phylogenetic tree, it is conceivable that other mycobacteria are also
273   capable of forming CWD cells such as *Mycobacterium abscesses*, *Mycobacterium*
274   *ulcerans* and *M. tuberculosis* (Fig. 4E). Remarkably, *M. marinum* and *M. bovis* BCG
275   strains only formed CWD cells in response to cell wall-targeting antibiotics, indicating
276   that the integrity of the cell wall of these strains is intrinsically stronger compared to
277   other non-tuberculosis mycobacteria (NTM). Perhaps this increased cell wall integrity
278   is due, at least in part, to the presence of methyl-branched fatty acids-containing lipids,
279   such as phthiocerol dimycocerates (PDMIs), that are unique to these pathogenic
280   mycobacteria (Yu *et al.,* 2012). The role of increased cell wall integrity, however, in
281   terms of mycobacterial morphological plasticity and virulence needs to be further
282   elucidated.

283   In conclusion, our work shows that mycobacteria form viable CWD cells in
284   response to environmental stressors and that this response is reversible. CWD cells
285   are undetectable by classical diagnostic approaches and in all likelihood have
286   therefore been over-looked in clinical settings. It is advisable to revisit current
287   diagnostic approaches to ensure proper detection of CWD cells. Potentials in future
288   detection of mycobacterial CWD cells could, for example, involve targeting
289   mycobacterial specific plasma membrane components, such as phosphatidylinositol
290   dimannosides (PIM2) (Sohlenkamp and Geiger, 2016). As some of the most important
291   antigens of mycobacteria are cell wall-associated glycolipids and lipoproteins, the loss
292   of the cell wall would potentially allow such cells to escape from recognition by the
293   host immune system, further contributing to host persistence (Källenius *et al*., 2016).
294   Their role in mycobacterial pathogenesis deserves more in depth attention. If indeed
295   CWD cells are a major contributor to bacterial persistence, further studies are needed
296   to investigate their role in the pathogenesis of (chronic and recurring) mycobacterial
297   infections, as well as to provide important new leads for discovery and development
298   of better antimicrobial agents to combat the devastating diseases caused by these
299   bacteria.

300

MATERIAL AND METHODS

Mycobacterial strains and culture conditions

All Mycobacterium used in this study are listed in Table S1. Unless stated otherwise, the strains were cultured on Middlebrook 7H10 agar (BD Difco) supplemented with 0.5 % (vol/vol) glycerol (Duchefa G1345) and 10 % (vol/vol) Middlebrook oleic acid-albumin-dextrose-catalase (OADC; BD BBL) added before and after autoclavation, respectively. For growth in liquid, the strains were cultivated in Middlebrook 7H9 broth (BD Difco) supplemented with 0.2% (vol/vol) glycerol and 10 % (vol/vol) albumin-dextrose-catalase enrichment (ADC; this lab) added before and after autoclavation, respectively. The ADC enrichment was made following the composition of the BD BBL ADC enrichment, containing per litre 8.5 g sodium chloride (Sigma-Aldrich 31434), 50 g Bovine Serum Albumin heat shock fraction (BSA; Sigma-Aldrich A9647), 20 g D-glucose (Duchefa G0802) and 0.03 g Catalase from bovine liver (Sigma-Aldrich C9322). The plasmid pCHERRY10 was obtained from Addgene (#24664), to fluorescently label *M. smegmatis* mc^{2}155 with mCherry under the constitutively G13 promoter. To culture the fluorescent strain, the antibiotic hygromycin B (Duchefa) was added to a final concentration of 100 μg·mL^{-1}. *M. marinum* and mycobacterial endophytes were cultivated at 30 °C at 200 rpm and 100 rpm, respectively. The remaining mycobacterial strains were grown at 37 °C, with an agitate on speed of 200 rpm. To obtain exponential growing cells of *M. smegmatis* mc^{2}155, the strain was inoculated from a colony and precultured in 10 mL MB7H9 (Erlenmeyer flask; 50 mL) to stationary phase. This preculture was diluted 1000-fold in 50 mL MB7H9 in 250 mL coiled Erlenmeyer flasks, resulting into exponential grown cells after 16 - 24 hours, with an OD$_{600nm}$ = 0.4 – 1.0.

To support growth of mycobacterial CWD cells, the strains were grown in media previously used for cultivating CWD cells of filamentous actinobacteria (Ramijan *et al*. 2018). Adjusted solid L-Phase Medium Agar (LPMA) contains 0.5 % D-glucose (w/v), 0.5 % Yeast Extract (w/v) (Gibco™), 0.5 % Bacto™ Peptone (w/v) (Gibco™), 0.58 M Sucrose (w/v) (Duchefa S0809), 0.01 % MgSO4·7H2O (w/v) (Sigma-Aldrich 10034-99-8) and 0.75 % Iberian agar (w/v), supplemented with 5 % Horse Serum (v/v). Standard adjusted liquid L-Phase Broth (LPB) medium is composed of yeast extract (w/v), 0.25 % Bacto™ Peptone (w/v), 0.15 % Malt Extract (w/v) (Duchefa M1327), 0.5 % D-glucose (w/v), 1.5% Bacto™ Tryptic Soy Broth (w/v) (BD™ 211825) and 0.64 M

334   Sucrose. Cultures were incubated either at 30 °C or 37 °C, while slowly shaking at 100

335   rpm.

336   To investigate the effect of the sucrose concentration on bacterial growth and

337   extrusion of CWD cells, LPB medium with different amounts of sucrose were prepared

338   (ranging from 0-1.0 M sucrose). For the detection of CWD cells, *M. smegmatis*

339   Mc^{2}155::pCHERRY10 was grown to exponential phase, as described, and inoculated

340   in Erlenmeyer flasks containing 10 mL LPB supplemented with the sucrose gradient

341   to an high optical density (final OD_{600nm} = 0.1) in duplicate. After 16 hours, the presence

342   of CWD cells was analysed by phase contrast microscopy and quantified by flow

343   cytometry, as described below. To assess bacterial growth, the same exponential

344   phase grown Mc^{2}155::pCHERRY10 was inoculated with low turbidity (final OD_{600nm} =

345   0.01) in a flat polystyrene 96-well plate ([GRE96ft] - Greiner 96 Flat Transparent Cat.

346   No.: 655101/655161/655192) containing 200 μL standard LPB supplemented with

347   sucrose in triplicates. Growth output was assessed through OD_{600nm} measurements in

348   technical duplicates using a TECAN Spark® 10M with SparkControl (v 2.3) software.

Enrichment of CWD cells

350   To enrich for mycobacterial CWD cells, *M. smegmatis* was grown to exponential phase

351   as described, inoculated to an high cell density (OD_{600nm} = 0.1) in 100 mL standard

352   LPB or LPB with 1.0 M sucrose and incubated at 37 °C, while shaking at 100 RPM.

353   CWD cells were filtered through a 11 μm pore size cellulose Whatman™ filter (Sigma

354   Aldrich, WHA1001055), utilizing a 47 mm Magnetic Filter Funnel (VWR 516-7597) and

355   a vacuum pump, and enriched by centrifugation of the supernatant for 1 hour at 1000

356   x g. Finally, cells were resuspended into 1-5 mL of the remaining supernatant.

Generation of protoplasts

358   To obtain mycobacterial protoplasts, a protocol was developed based on existing

359   protocols used to generate protoplasts in *Streptomyces* (Kieser, 2000) and

360   spheroplasts in Mycobacteria (Udou, 1982). In short, cells were grown to exponential

361   phase (OD_{600nm} = 0.4) in standard MB7H9, after which 1 % glycine (Duchefa) was

362   added followed by growth for another 16-24 hours. Cells were harvested at 4000 x g

363   for 10 min and 2x washed at 1200 x g for 14 min in Sucrose Magnesium (SM) solution

364   (10.3 % sucrose (w/v) and 25 mM $MgCl_2$ (Duchefa M0533) in MQ). Cells were then

365   resuspended in Lysozyme solution (pellet of 20 mL starting culture in 4 mL solution),

366　containing 1 mg·mL^{-1} Lysozyme (Sigma-Aldrich 62971) in protoplast buffer as

367　described in Kieser, and incubated at 37 degrees while standing for 16-20 hours.

368　Briefly, basic protoplast buffer is prepared by adding 10.3 g Sucrose, 25 mg K_2SO_4,

369　0.202 g $MgCl_2·6H_2O$ and 200 μL trace elements in 80 mL MQ and autoclave for 20

370　min at 120 °C. Trace elements consist of (L^{-1}) 40 mg $ZnCl_2$, 200 mg $FeCl_3·6H_2O$, 10

371　mg $CuCl_2·2H_2O$, 10 mg $MnCl_2·4H_2O$, 10 mg $Na_2B_4O_7·10H_2O$ and 10 mg

372　$(NH_4)_6Mo_7O_{24}·4H_2O$. Protoplast buffer then is enriched with 1 mL KH_2PO_4 (0.5%), 10

373　mL $CaCl_2·2H_2O$ (5M, 3.68%) and 10 mL TES buffer (5.73%, 0.25 M, pH 7.2).

374　Successful protoplasting was monitored using phase contrast microscopy. After

375　protoplasts were formed, cell debris was removed by filtration through a SM

376　prewashed 40 μm cell strainer (PluriStrainer® SKU 43-50040-51).

377

378　**Light microscopy**

379　To immobilize cells, unless stated otherwise, basic LPM agar pads lacking horse

380　serum were made utilizing a 15 mL falcon tube on a thin layer agar plate. Alternative,

381　ultrapure MilliQ (MQ) water containing 1.5 % agarose with or without supplementation

382　of 30 % sucrose was used to generate pads. For imaging, 5 μL of sample was either

383　loaded on an agar pad placed on a glass slide (Fisher 1157-2203) and covered with

384　20 x 20 mm (Epredia #1) coverslip, or directly loaded in a 35 mm imaging μ-dish

385　(Ibidi®) and covered by an agar pad. Phase contrast images were obtained using a

386　Zeiss Axio Lab A1 upright microscope equipped with a Zeiss Axiocam 105 color

387　(resolution 5 mega pixel, 2.2 μm/pixel) and collected using Zen 2 software (blue

388　edition, Carl Zeiss Microscopy GmbH). Differential Interference Contrast (DIC), phase

389　contrast and fluorescent images were taken with a Zeiss Axioplan 2 upright

390　microscope equipped with an Axiocam Mrc 5 camera utilizing AxioVison Rel. 4.8.1.0

391　Zen software (Carl Zeiss Imaging Solutions GmbH). Fluorescent filter sets applied

392　were 63 HE (Carl Zeiss, consisting of a 572/25 bandpass excitation filter, 590nm beam

393　splitter, and 629/62 nm bandpass emission filter) to capture mCherry fluorescence.

394　Fluorescent live imaging was performed on a Zeiss AXIO Observer.Z1 equipped with

395　a Hamamatsu ImagEM X2 EM-CCD camera C9100 utilizing Zen 2.6 software (blue

396　edition, Carl Zeiss Microscopy GmbH). Confocal images were acquired with a Zeiss

397　LSM 900 confocal microscope with Airyscan 2 module, temperature control chamber

398　and Zen 3.1 software (blue edition, Carl Zeiss Microscopy GmbH). All excitation and

399 emission settings for this microscope are listed in Supplemental Table S2. Microscopy

400 images were processed using either OMERO or ImageJ/FIJI (Schindelin *et al*., 2012).

Fluorescent probes

402 Fluorescent probes were added to 25 μL aliquots of liquid cultures or resuspended

403 colonies, followed by incubation at room temperature for 15 min. Nucleic acids were

404 stained using 2 μM SYTO 9 (S34854, Invitrogen). The plasma membrane was labelled

405 using SynapseRed C2M (SynapseRed, PK-CA707-70028, PromoKine, PromoCell

406 GmbH; also known as FM5-95, a trademark of Molecular Probes, Inc.) to a final

407 concentration of 70 μM.

Cell diameter measurements

409 Cell diameters of extruded CWD *M. smegmatis* mc^{2}155 cells, grown in LPB

410 supplemented with 1.0 M sucrose in triplicate, were measured overtime by fluorescent

411 labelling of cell membranes with SynapseRed through confocal micrograph

412 acquisitions. Spherical structures that were not positively labelled with SYTO 9, and

413 therefore lacking nucleic acids, were excluded from the assessment. Micrographs

414 were analysed using FIJI/ImageJ (Schindelin *et al.,* 2012).

Flow cytometry

416 To quantify walled and CWD cells, flow cytometry was used. Briefly, red fluorescent

417 *M. smegmatis* mc^{2}155::pCHERRY10 cells were filtered through a LPB prewashed 40

418 μm cell strainer (PluriStrainer® SKU 43-50040-51) prior to quantification using a Bio-

419 Rad S3e Fluorescence-activated Cell Sorter (FACS) equipped with ProSort™

420 Software, version 1.6. Fluorescence was detected following excitation at 561 nm and

421 by using a 615/25 nm bandpass emission filter (FL3). As sheath fluid, ProFlow Sort

422 Grade 8x Sheat Fluid (Bio-Rad Laboratories, inc; #12012932) was used. Quality

423 control (QC) was passed utilizing ProLine™ Universal Calibration Beads (Bio-Rad

424 Laboratories, inc; #1451086). The threshold was set on 0.02 FCS to minimize

425 background noise and the flow was adjusted to 500 events per second. For the

426 sucrose gradient 50,000 events were collected. For the triton viability assay, 20,000

427 events were collected and experiments were performed in triplicate. All data analysis

428 was done using FlowJov10.8.1 (BD BioSciences). To remove outliers, three

429 successive gates were drawn in $1.1 \cdot 10^0$ Side Scatter (SSC) x $1.1 \cdot 10^0$ Forward

430 Scatter (FSC) Height, 1.5K - 2.5K SSC Width x Height and 1.5K-2.5K FSC Width x

14

431   Height, respectively (Fig. S2). iQuadrant bins were drawn to roughly distinguish walled

432   and CWD cells, typically $2 \cdot 10^1$ SSC Height over $1 \cdot 10^1$ FL3 (Sucrose gradient &

433   Protoplasts) and $5 \cdot 10^1$ SSC Height over $4 \cdot 10^1$ FL3 (Triton viability) to select for

434   complexity and fluorescence. Specific gates were drawn to include populations of

435   interest in SSC x FL3, including subpopulations in lower sucrose conditions of

436   propagating walled cells. Relative population percentages represented by the

437   populations "Walled fluorescent" and "CWD fluorescent" were not further utilized for

438   analysis. Biological and technical replicates were separately processed for graphical

439   representation and concatenated for statistical analysis and visualization purposes.

440   Pearson Chi-squared were performed on detergent treatment compared to expected

441   no treatment within separate iQuadrant bin populations (df = 2) or over the total

442   iQuadrant bins population (df = 4), as found in Supplemental Table 3.

Cryo-Transmission Electron Microscopy

444   Mycobacterial cells were prepared and checked by phase contrast for cell morphology

445   and cell density. From the prepared cells, 20 μL samples were mixed with 2 μL 10 nm

446   colloidal gold beads (Protein A coated, CMC Utrecht), of which 3-4 μL was applied on

447   glow-discharged 200 mesh copper grids with an extra thick R2/2 carbon film (Quantifoil

448   Micro Tools). Vitrification was performed using an automated Leica EM GP plunge-

449   freezer, which automatically pre-blots for 30 seconds, followed by 1 second blotting

450   step and plunge-freezing of the grid into liquid ethane. The samples were mounted on

451   a 626 cryo-specimen holder (Gatan, Pleasanton, CA) and imaged using a 120 kV

452   Talos TEM (Thermo Fisher Scientific) equipped with a Lab6 electron emission source

453   and Cita detector (Thermo Fisher Scientific). The resulting Cryo-TEM micrographs

454   have a pixel size of 0.34 nm·pixel^{-1}. The density plots of the mycobacterial cell

455   envelope were generated through FIJI/ImageJ (Schindelin *et al.,* 2012).

Viability assay

457   To test the viability of mycobacterial CWD cells, the pCHERRY10 expressing *M.*

458   *smegmatis* mc^{2}155 cells were exposed to the detergent Triton x-100 (TX-100)

459   (PanReac AppliChem) and plated on MB7H10 medium to detect colony forming units

460   (CFU). CWD cells were generated as described and enriched after three days of

461   growth. As a walled control, the cells were grown in MB7H9 to exponential phase in

462   24 hours. As a control, protoplasts were generated as described above. The cells were

463   then exposed for 15 min to either MilliQ (MQ) or 0.1% MQ + TX-100. To detect viable

464   CFUs, the samples were 10-fold diluted in LPB (20 μl in 180 μl) in polystyrene 96-well

465   plate utilizing multichannel pipets. 10 μl spots of diluted samples were plated in

466   duplicate on MB7H10, dried for 15 min and incubated for 5 days at 37 °C. After

467   spotting, the cells were inspected through flow cytometry and DIC-fluorescence for the

468   presence of spherical mCherry-expressing cells. Paired student t-tests were

469   performed were performed on TX-100 treatment compared to no treatment, as found

470   in Supplemental Table 4.

Antibiotic CWD induction assay

471

472   Minimal inhibitory concentration (MIC) assays were performed to detect their effect on

473   the formation of CWD cells. For this, 2-fold dilutions of antimicrobial agents in MB7H9,

474   LPB 0 M sucrose and LPB 0.4 M sucrose were prepared in polystyrene 96-wells plate

475   ([GRE96ft] - Greiner 96 Flat Transparent Cat. No.: 655101/655161/655192), including

476   starting concentrations (w/v): 50 mg·mL^{-1} isoniazid (Duchefa), 50 mg·mL^{-1} D-

477   cycloserine (Duchefa) and 5 mg·mL^{-1} vancomycin (Duchefa). MIC assays were

478   performed in triplicate and contained a Blanco measurement per concentration.

479   Exponential growing *M. smegmatis* mc^{2}155::pCHERRY10 cells were inoculated at a

480   turbidity of OD$_{600nm}$= 0.01, incubated 100 RPM for 7 days. Incubation was performed

481   at 30 °C and wrapped in parafilm to reduce well evaporation. Output was assessed

482   through turbidity measurements using a TECAN Spark$^®$ 10M with SparkControl (v 2.3)

483   software and by scanning the plates. Based on the MICs, antibiotic CWD induction

484   assays were reproduced in Erlenmeyer flasks containing 10 mL LPB with 0 or 0.4 M

485   sucrose supplemented with antibiotics, including 16 μg·mL^{-1} isoniazid, 16 μg/mL

486   vancomycin and 400 μg·mL^{-1} D-cycloserine. Controls included supplementation with

487   either 1 mg·mL^{-1} Lysozyme + 25 mM MgCl$_2$ (positive control) or no supplementation

488   (negative control). To test other mycobacterial species, all the antibiotic concentrations

489   were increased to 500 μg·mL^{-1} to overcome species-specific antibiotic MICs and to

490   ensure antibiotic effectiveness. All CWD induction assays were inoculated in high

491   turbidity of OD$_{600nm}$= 0.1 and grown 5-8 days at 30 or 37 °C 100 RPM mL. Non-

492   fluorescent strains were checked by phase contrast microscopy and subjected to

493   fluorescent dyes to assess the presence of nucleic acids and membranes by confocal

494   microscopy.

Phylogenetic analysis

For DNA isolation of strains that had not been sequenced, colonies were harvested from fresh agar plates. Samples were washed 3 times with sterile PBS and snap frozen. DNA was subsequently isolated using the method of Bouso *et al.* (2019) without shearing. For the library/run mode, the PromethION SQK-LSK109 ligation sequencing kit was used. Samples were run on an ONT GridION by FG-technologies, Leiden, The Netherlands. Base calling was done using Gupy v4.0.11. The sequencing data are available under NCBI submission number PRJNA895223. Genome sequences were used to construct a maximum-composite likelihood phylogeny tree using PhyloPhlAn (Segata *et al.,* 2013). Ortholog identification and alignment was performed in Phylophlan using the "-u" command. The phylogenetic tree was visualized using iTOL (Letunic and Bork, 2007). Reference genomes are listed in Supplemental Table 6.

Quantification of osmolality and osmotic pressure

To test conventional mycobacterial culture medium in their ability to sustain CWD cells, ascending sucrose amounts were added to conventional Middlebrook 7H9 and LPB media. Osmolality of the media was measured in sextuplicate using freezing point depression with an osmometer (Micro-Osmometer Autocal Type 13, Roebling), calibrated using distilled water (0) and 300 mOsm standard ampulla delivered with the instrument. To calculate the osmotic pressure (π) the following equation was applied: *π (mmHg) = 19.3 x osmolality (mOsm·kg^{-1})* (Rasouli, 2016). The mean values are listed in Table S7. To test the sustainability of CWD cells, *M. smegmatis* mc^{2}155 was grown to exponential phase, inoculated in the media with high turbidity (OD_{600nm}= 0.1) and exposed to 1 mg·mL^{-1} lysozyme and 25 mM $MgCl_2$ for 24 hours at 37 °C at 100 rpm. The conditions were screened for the presence of spherical cells by phase contrast microscopy.

Mycobacterial diagnostics

Conventional carbol fuchsin staining was performed using hot Ziehl-Neelsen complete staining kit (CLIN-TECH limited product code 62103, BioTrend) (Ziehl, 1882; Neelsen, 1883). In short, the stain was prepared as follows: 1) 100 μL of cells were spread and airdried on glass slides. 2) The cells were fixated by passing the glass slides 3 times through the flame. 3) The glass slides were flooded with carbol fuchsin (ZN) and heated above the flame until steam raised. 4) Slides were washed with demineralized

17

528   water. 5) 3 % alcohol acid (hydrochloric acid) was applied until no changes in color

529   occurred anymore. 5) The glass slides were rinsed with demineralized water and

530   counter stained with 0.05 % methylene blue for 10 seconds. 6) Slides were rinsed with

531   water, drained and airdried. 7) Slides were examined using oil immersion. Alternative

532   carbol fuchsin staining was performed using cold Kinyoun staining (CLIN-TECH limited

533   product code 621045, BioTrend) (Kinyoun, 1915). In short, this stain was prepared as

534   follows: 1) 100 µL of cells were spread and airdried on glass slides. 2) The cells were

535   fixated by passing the glass slides 3 times through the flame. 3) The glass slides were

536   flooded with carbol fuchsin (Kinyoun's) for 1 minute. 4) Slides were gently washed with

537   demineralized water. 5) 3 % alcohol acid was applied until no changes in color

538   occurred anymore, in less than 30 seconds. 5) The glass slides were directly rinsed

539   with demineralized water and counter stained with 0.05 % methylene blue for 30

540   seconds. 6) Slides were rinsed with water, drained and air-dried. 7) Slides were

541   examined with DIC microscopy using oil immersion.

ACKNOWLEDGEMENTS

AUTHOR CONTRIBUTIONS

551   N.D. and T.W. carried out the experiments. V.C.B. constructed the phylogenetic tree,

552   while H.P.S. sequenced the Mycobacterial genomes. All authors contributed to the

553   experimental design and discussion of results. N.D and D.C wrote the manuscript with

554   input from all authors.

555

DECLARATIONS OF INTEREST

557   The authors declare no competing interests.

558

FIGURES LEGENDS

Figure 1. Hyperosmotic stress causes cell wall-deficiency in mycobacteria.

A) Plate scans, stereo images and phase contrast micrographs of *M. smegmatis* mc^{2}155 colonies grown for 3 days on standard cultivation medium MB7H10 or for 6 days on hyperosmotic LPMA medium. Scale bar represents 50 mm and 10 μm.

B) DIC and fluorescent micrographs of *M. smegmatis* mc^{2}155 grown for 3 days on MB7H10 and LPMA plates and in liquid LPB medium. Nucleic acids were labeled with SYTO 9 for 15 min. Scale bars represent 10 μm.

C) Confocal image of a nucleic acid-containing cell of *M. smegmatis* mc^{2}155 fluorescently labeled with pCHERRY10 (Caroll *et al.,* 2010) after 10 days of growth in LPB medium. Nucleic acids were labeled with SYTO 9 for 15 min. Scale bar represents 2 μm.

D) Confocal images of *M. smegmatis* mc^{2}155 cells with different diameters, 1.8 μm and 6.8 μm, respectively, formed in LPB medium. Membranes were labeled with SynapseRed for 15 min. Scale bars represent 5 μm.

E) Stills of *M. smegmatis* mc^{2}155 showing extrusion of CWD cells in LPB medium. Scale bars represent 5 μm.

F) Phase contrast micrographs of *M. smegmatis* mc^{2}155::pCHERRY10 grown in ascending concentrations of sucrose for 1 day. Scale bars represent 10 μm.

G) Correlation between optical density and the number of CWD cells of *M. smegmatis* mc^{2}155::pCHERRY10 in LPB supplemented with ascending concentrations of sucrose. The number of CWD cells is represented as the percentage of all cells in the cultures, which was quantified using flow cytometry (See Figs. S1E and S2). Optical density measurements (OD$_{600nm}$) was were performed over time as shown in Supplemental Figure S1F.

H) Confocal images of mycobacterial strains grown in LPB supplemented with 1.0 M sucrose. Images were made after 2 days (*M. smegmatis* strains) or 2 weeks (*Mycobacterium avium* complex (MAC) strains). Nucleic acids and cell membrane were labeled with SYTO 9 and SynapseRed, respectively, for 15 min. Scale bars represent 2 μm.

Figure 2. Wall-deficient cells of *M. smegmatis* lack major cell wall components.

A) Cryo-Transmission Electron Microscopy (TEM) images of walled cells, CWD cells or protoplasts of *M. smegmatis* mc^{2}155. Walled cells were grown in MB7H9 liquid medium and blotted directly from culture. CWD cells were enriched after 8 days of growth in LPB 1.0 M sucrose. Protoplasts were generated by lysozyme treatment in P-buffer through an adjusted mycobacterial protoplast protocol (see Material and Methods). Scale bars represent 200 nm. The lower panels represent zoomed in areas and scale bars correspond to 150 nm. CM, cytoplasmic membrane; MOM, mycobacterial outer membrane (Sani *et al.,* 2010).

B) Gray scale density plot measurements from zoomed-in Cryo-TEM micrographs across the cell envelope in right-angle (90°). CM, cytoplasmic membrane; L1 and L2, domain-rich periplasmic layers; MOM, mycobacterial outer membrane (Hoffmann *et al.,* 2008).

C) Cell envelope measurements based on density plots of selected cells (n = 6). Measurements were performed in duplicate at different locations per cell. The envelope diameter of CWD cells and protoplasts were measured in duplicate per cell (in 90° angle) and the walled cells were measured at the tip and at the side wall in relative distance from the tip curvature.

D) Cell diameter measurements of selected cells (n=6). The diameter was measured in duplicate per cell, in perpendicular for spherical cells (CWD cells and protoplast) and perpendicular to the longitudinal axis of the rod shaped cell (side to side walls), with an minimum of 50 nm distance (Walled).

Figure 3. Wall-deficient cells of *M. smegmatis* are viable.

A) Phase contrast and fluorescent images of *M. smegmatis* mc^{2}155::pCHERRY10 walled cells, CWD cells and protoplasts after exposure to detergent 0.1% Triton X-100 (TX-100) for 15 min. As a control MQ was added to the cells. Scale bars represent 10 μm.

B) Time-lapse images of *M. smegmatis* mc^{2}155::pCHERRY10 exposed to 0.1 % TX-100. Please note that walled cells, indicated with arrows, do not disappear over time in contrast to CWD cells. Scale bars represent 50 μm. Time is indicated in hours.

622   **C)** Flow cytometry plots of M. smegmatis mc^{2}155::pCHERRY10 walled and CWD
623   cells in response water (control) or t Triton X-100 exposure (TX-100) in triplicates.
624   Plots were divided in four quadrants representing Highly complex, non-fluorescent
625   particles (Q1), Highly complex fluorescent particles (Q2, Walled cells), Less
626   complex, fluorescent particles (Q3, CWD cells), and Less complex, non-
627   fluorescent particles (Q4). Please note that the CWD cells disappear when treated
628   with TX-100 (right panels).

629   **D)** Quantification of flow cytometry data. White bars represent walled cells, while light
630   grey and dark grey represent non-fluorescent particles and CWD cells,
631   respectively. Please note that the addition of TX-100 (T), in contrast to the water
632   control (C), dramatically reduces the number of CWD cells and protoplasts, while
633   having no effect on the walled cells. All measurements were performed in triplicate
634   (see Fig. S6).

635   **E)** Quantification of Colony Forming Units (CFU) counts of walled cells, CWD cells
636   and protoplasts after the exposure to TX-100 (T) or water (C). Colonies were
637   counted after 3 days. All measurements were performed in triplicate.

638

639   **Figure 4. Cell wall-targeting antibiotics induces wall-deficiency in mycobacteria.**
640   **A)** Images of *M. smegmatis* mc^{2}155::pCHERRY10 after 7 days of growth in the
641   presence of 6 μg·mL^{-1} isoniazid, 195 μg·mL^{-1} D-cycloserine or 1.2 μg·mL^{-1}
642   vancomycin. The control shows growth without the addition of antibiotics. CWD
643   cells are indicated by arrows. Scale bars represent 10 μm.

644   **B)** Confocal images showing CWD cells of *M. smegmatis* mc^{2}155 formed after 5 days
645   of growth in LPB (0.4 M sucrose) supplemented with 16 μg·mL^{-1} vancomycin.
646   Nucleic acids and cell membranes were labeled with SYTO 9 and SynapseRed,
647   respectively. CWD cells are indicated by arrows. Scale bars represent 5 μm.

648   **C)** Phase contrast micrographs of *M. bovis* BCG Russia, *M. marinum* M and *M. avium*
649   strains MAC101 and Vet. 1387 exposed to 500 μg·mL^{-1} D-cycloserine in LPB 0.4
650   M sucrose for 8 days. Scale bars represent 5 μm.

651   **D)** Confocal images of DNA containing CWD cells of *M. bovis* BCG Russia and *M.*
652   *marinum* M, formed after 8 days of growth in LPB (0.4 M sucrose) supplemented
653   with 500 μg·mL^{-1} D-cycloserine. Nucleic acids and cell membranes were labeled
654   with SYTO 9 and SynapseRed, respectively. Scale bars represent 2 μm.

E) Phylogenetic tree of mycobacteria based on whole genome sequences. Asterisk(s) indicate strains tested in this study with the natural ability to form CWD cells in the absence (**) or in the presence (*) of antibiotics. Strains that were "not tested" are indicated with the designation NT. As outgroup *Corynebacterium* was included, which was shown to be capable of propagating as an L-form (Mercier *et al.,* 2014). Reference genomes are listed in Supplemental Table 6.

Figure 5. CWD cells of mycobacteria are undetectable by conventional diagnostics.

A) Phase contrast images of *M. smegmatis* mc^{2}155 after exposure to 1 mg·mL^{-1} lysozyme for 24 hours in MB7H9 supplemented with or without 0.2 M sucrose. The presence of CWD cells are indicated by arrows. Scale bars represent 5 μm.

B) Osmolality measurements of MB7H9 supplemented with or without 0.2 M sucrose. Measurements were performed in sextuplicate.

C) Images of *M. smegmatis* mc^{2}155::pCHERRY10 CWD cells formed in LPB (1.0 M sucrose) mounted on MQ and MQ/sucrose (0.8 M) agar pads. Please note that all CWD cells are absent when placed on MQ agar pads. Scale bars represent 10 μm.

D) DIC images of conventional Ziehl-Neelsen staining and Kinyoun staining on *M. smegmatis* mc^{2}155::pCHERRY10 walled and enriched CWD cells. Acid fast bacteria (AFB) stain (positively) red, while the blue color indicates "background". Phase contrast images were taken before the staining procedure. Please note that the fluorescent (CWD) cells are visible in the region of interest (ROI), which, however, do not stain red. CWD cells are indicated by arrows. Scale bars represent 10 and 5 μm.

E) Schematic model representing the application of Ziehl-Neelsen staining on walled and CWD mycobacteria in hypo- (left) and hypertonic (right) conditions. Please note that wall-targeting agents further stimulate the formation of CWD cells, which remain undetected by this staining method. Created with BioRender.com.

SUPPLEMENTAL FIGURES LEGENDS

Figure S1. Formation of CWD cells in *M. smegmatis* containing DNA.

A) Confocal images of nucleic acid containing CWD cells from *M. smegmatis* mc^{2}155 with relative large diameters formed overtime in LPB. Nucleic acid and membrane

688 were labeled with SYTO 9 and SynapseRed, respectively. Scale bars represent 2

689 μm.

690 B) Image of *M. smegmatis* mc^{2}155 walled cells and CWD cells grown for 10 days in

691 LPB (1.0 M sucrose). Nucleic acid and membrane were labeled with SYTO 9 and

692 SynapseRed, respectively. Scale bar represent 5 μm.

693 C) Cell diameter measurements of nucleic acid containing CWD cells over time (n =

694 480-684 per time point, single measurement per CWD cell). Graph represents

695 measured means and standard deviation.

696 D) Confocal Z-stack images of *M. smegmatis* mc^{2}155::pCHERRY10 CWD cell grown

697 10 days in LPB. Nucleic acids were labeled with SYTO 9 for 15 min. Confocal

698 images were taken in 8 times Z-stacks of 270 nm. Scale bar represents 5 μm.

699 E) Quantification of flow cytometry data (see Fig. S2) of *M. smegmatis*

700 mc^{2}155::pCHERRY10 grown for 2 days in LPB containing various concentrations

701 of sucrose. White bars represent walled cells, while light grey and dark grey

702 represent non-fluorescent particles and CWD cells, respectively. Please note that

703 increasing the concentration of sucrose results in a higher number of CWD cells.

704 F) Growth curve based on optical density measurements (OD$_{600nm}$) of *M. smegmatis*

705 mc^{2}155::pCHERRY10 grown for 4 days in LPB containing various concentrations

706 of sucrose. Please note that increasing the concentration of sucrose, results in the

707 inhibition of growth.

708

709 **Figure S2. Flow cytometry processing of fluorescent labelled walled and CWD**

710 **cells of *M. smegmatis***

711 Flow cytometry gating workflow for remove outliers and select populations of interest.

712 **A)** Removal of outliers represented by the two extremity conditions, LPB

713 supplemented with 0 M and 1.0 M sucrose. Gate 1 in the FSC x SSC Height log,

714 to remove background outliers present on both axis. Gate 2 in the SSC Height x

715 Width log to remove outliers in the SSC. Gate 3 in the FSC Height x Width log to

716 remove outliers in the FSC. Populations represented in SSC x fluorescent filter 3

717 (FL3), bandwidth 615/25 with laser 56.1 Simple iQuadrants bins gating for

718 estimated separation of populations, namely Highly complex, non-fluorescent

719 particles (Q1), Highly complex, fluorescent particles (Q2, Walled), Less complex,

720   fluorescent particles(Q3, CWD cells), and Less complex, non-fluorescent particles

721   (Q4).

722   **B)** Specific gates drawn to specific populations of interest in SSC x FL3, including

723   subpopulations in lower sucrose conditions of propagating walled cells with

724   nascent, less complex, cell walls prior cell wall modifications. Relative population

725   percentages represented by the populations "Walled fluorescent" and "CWD

726   fluorescent".

727

728   **Figure S3. CWD formation in response to hyperosmotic conditions in various**

729   **mycobacterial species**

730   Confocal micrographs of various mycobacterial strains grown in LPB (1.0 M sucrose).

731   Cells were fluorescently dyed with SYTO 9 and SynapseRed to label nucleic acids

732   and membranes, respectively.

733   **A)** Mycobacterial strains were grown for either 2 days (*M. smegmatis* strains) or 2

734   weeks (*Mycobacterium avium* complex strains) at 37 °C 100 RPM, or were grown

735   1 week at 30 °C 100 RPM (endophytic isolates). Scale bars represent 2 μm.

736   **B)** Veterinary isolate *Mycobacterium avium* subsp. *hominissuis* 20-935 /2 grown for 2

737   weeks at 37 °C 100 RPM. Please note that this strain produces some CWD cells,

738   but mostly empty membrane vesicles. Scale bar represent 10 μm.

739

740   **Figure S4. Enrichment of mycobacterial CWD cells**

741   **A)** Enrichment method of CWD cells utilizing particle retention of 11 μm and slow

742   centrifugation. In short, CWD cells are produced in as described in Material and

743   Methods. Incubate until CWD cells are formed and filter culture with vacuum pump.

744   Centrifuge filtrate for 1 hour at low centrifuging force (1000 x g). Please note that

745   low centrifuging force is needed to avoid cell shearing of the sensitive CWD cells.

746   Resuspend loose pellet in left-over supernatant. Created with BioRender.com.

747   **B)** Phase contrast images of *M. smegmatis* mc^{2}155 CWD cells grown for 8 days in

748   LPB (1.0 M sucrose), before and after enrichment. Scale bars represent 50 μm.

749

Figure S5. Cryo-TEM images of various cells of *M. smegmatis*.

A) Cryo- TEM images of exponential-phase grown *M. smegmatis* mc^{2}155 in MB7H9 liquid media, blotted directly from culture. Selected walled cells used for analysis. Scale bars represent 1 μm, 2 μm, 200 nm or 100 nm.

B) Cryo-TEM micrographs of *M. smegmatis* mc^{2}155 enriched CWD cells, grown 8 days in LPB 1.0 M Sucrose. Selected CWD cells used for analysis. Scale bars represents 1 μm, 200 nm or 100 nm.

C) Cryo-TEM micrographs of *M. smegmatis* mc^{2}155 artificial produced protoplasts in P-buffer. Selected protoplasts used for analysis. Scale bars represents 1 μm or 200 nm.

D) Cryo-TEM micrograph region of interest in shows wall-like structures detected on top of plasma membrane of *M. smegmatis* mc^{2}155 enriched CWD cell, indicated by arrow. Density plot of 150 nm across cell membrane shows an extra depth representing the wall-like structure, measuring an increase in cell-envelope size to 15.77 nm. Scale bar represents 100 nm.

Figure S6. CWD cells are sensitive to detergent Triton X-100

A) Flow cytometry plots of M. smegmatis mc^{2}155::pCHERRY10 walled cells, either grown in MB7H9 or LPB (0.63 M sucrose), CWD cells, grown in LPB (1.0 M sucrose) and protoplasts (Lysozyme solution) exposed to water (control) or the detergent TX-100. Plots were divided in four quadrants representing Highly complex, non-fluorescent particles (Q1), Highly complex fluorescent particles (Q2, Walled cells), Less complex, fluorescent particles (Q3, CWD cells), and Less complex, non-fluorescent particles (Q4). Relative population percentages represented by the populations "Walled fluorescent" and "CWD fluorescent".

B) Quantification of flow cytometry data. White bars represent walled cells, while light grey and dark grey represent non-fluorescent particles and CWD cells, respectively. Please note that the addition of TX-100 (T), in contrast to the water control (C), dramatically reduces the number of CWD cells grown in LPB (1.0 M sucrose) and protoplasts (Lysozyme solution), while having no effect on the walled cells grown in MB7H9 and LPB (0.63 M sucrose).

C) Quantification of Colony Forming Units (CFU) counts of walled cells (MB7H9 or LPB 0.63 M sucrose), CWD cells (LPB 1.0 M sucrose) and protoplasts (Lysozyme

783   solution) after the exposure to TX-100 (T) or water (C). Colonies were counted after

784   3 days. All measurements were performed in biological triplicates and technical

785   duplicates.

786

787   **Figure S7. CWD formation in MIC assays of cell wall targeting antibiotics.**

788   MIC assays of *M. smegmatis* mc^{2}155::pCHERRY10 in response to isoniazid, D-

789   cycloserine and vancomyin in either MB7H9, LPB 0 M sucrose or LPB 0.4 M sucrose,

790   performed in 96-well plates. Biological replicates were applied. Data was collected

791   after 7 days. MIC determinations in hyperosmotic media are listed in Supplemental

792   Table 5.

793   **A)** Scanning images of the 96-well plates.

794   **B)** Optical density measurements of the MIC plates.

795   **C)** DIC-fluorescent images of walled and CWD cells. Please note that CWD cells are

796   solely observed in sucrose supplemented LPB in response to the presence of

797   antibiotics.

798

799   **Figure S8. Cell wall-targeting antibiotics induces the formation of CWD cells in**

800   ***M. smegmatis***

801   Phase-contrast images showing CWD cells of *M. smegmatis* mc^{2}155 formed in LPB

802   (0.4 M sucrose) in response to cell wall-targeting antibiotics. Controls includes 1

803   mg/mL lysozyme + 25 mM MgCl$_2$ (positive control) and no supplementation (negative

804   control).

805   **A)** Formation of CWD cells after 5 days exposure to either 16 μg·mL^{-1} isoniazid, 400

806   μg·mL^{-1} D-cycloserine or 16 μg·mL^{-1} vancomycin. Scale bars represent 10 μm.

807   **B)** Formation of CWD cells after 8 days exposure to elevated antibiotic

808   concentrations, namely 500 μg·mL^{-1}. Scale bars represent 5 μm.

809

810   **Figure S9. Cell wall-targeting antibiotics induces the formation of CWD cells**

811   **mycobacterial species**

812   Phase-contrast images of various mycobacterial strains grown in LPB (0.4 M sucrose)

813   supplemented with 500 μg·mL^{-1} of either isoniazid, D-cycloserine or vancomycin.

814   Controls includes 1 mg·mL^{-1} Lysozyme + 25 mM MgCl$_2$ (positive control) and no

815   supplementation (negative Control). Scale bars represent either 5 or 2 μm.

816   **A)** *M. avium* Complex (MAC) strains

817   **B)** *M. bovis* BCG strains

818   **C)** *M. marinum* M strain

819   **D)** Endophyte isolates

820

821   **Figure S10. CWD cells require osmolytes**

822   **A)** Phase contrast images of *M. smegmatis* mc^{2}155 exposed to 1 mg·mL^{-1} Lysozyme

823   + 25 mM MgCl2 for 24 hours in either MB7H9 or LPB supplemented with ascending

824   concentrations of sucrose. Scale bars represent 10 μm.

825   **B)** Osmolality measurements of LPB and MB7H9 with ascending concentrations of

826   sucrose. Original media includes standard used LPB at RT and MB7H9 kept at 4

827   °C. Measurements were performed in sextuplicate.

828   **C)** Phase contrast, DIC and fluorescent micrographs of *M. smegmatis*

829   mc^{2}155::pCHERRY10 walled grown in MB7H9 and CWD cells enriched from LPB

830   (1.0 M sucrose) mounted on MQ and MQ/sucrose (0.8 M sucrose) agar pads.

831   Please note that all CWD cells are absent when placed on MQ agar pads. Scale

832   bars represent 10 μm.

833

834   **SUPPLEMENTAL VIDEOS**

835   **Video S1. CWD cell extrusion at mycobacterial polar tips**

836   Confocal live imaging of *M. smegmatis* mc^{2}155 CWD cell extrusion overtime.

837   Exponential phase cells were grown in LPB for 6 hours prior imaging fixated under

838   LPMA agar pad. Scale bar represent 5 μm.

839

840   **Video S2. Explosive lysis of fluorescent CWD cells in response to TX-100**

841   **treatment**

842   Fluorescent live imaging of *M. smegmatis* mc^{2}155::pCHERRY10 CWD cells in

843   response to 0.1% TX-100 exposure. Scale bar represent 50 μm.

844   **SUPPLEMENTAL TABLES**

845   **Table S1.** Mycobacterial strains used

Strain	Genotype	Relevant description	Origin	Reference

M. smegmatis ATCC 607	wild-type	*M. smegmatis* (Trevisan 1889) Lehmann and Neumann 1899 (DSM 43465). Human isolation source. Low transformation efficiency and strong cell clumping.	DSM	Etienne *et al.,* 2005
M. smegmatis mc^{2}155	ept-1	Generally used mutated lab strain (ATCC 700084). Electro competent, loss of cell-clumping.	Wilbert Bitter	Snapper *et al.,* 1990
M. marinum M^{LU}	wild-type	*Mycobacterium marinum* Aronson M strain (ATCC BAA-535). Isolated from Human sample (Moffet Hospital # 975973)	Annemarie Meijer	Ramakrishnan and Falkow *et al.,* 1994
M. bovis BCG Pasteur	wild-type	*Mycobacterium bovis* Karlson and Lessel (ATCC 35734). Bacillus Calmette-Guérin (BCG) vaccine strain TMC 1011 [BCG Pasteur] (Pasteur 1173 P2)	ATCC	Oettinger *et al.,* 1999
M. bovis BCG Russia	wild-type	*Mycobacterium bovis* Karlson and Lessel (ATCC 35740). BCG vaccine strain TMC 1020 [BCG Russia] (Russia BCG-12)	ATCC	Oettinger *et al.,* 1999
M. avium MAC101	wild-type	*Mycobacterium avium* Chester strain 101 (ATCC 700898). Human isolation source.	ATCC	
M. avium Vet. 1387	wild-type	*Mycobacterium avium* supsp. *avium* Chester (ATCC 25291). Veterinary isolation strain Vet. 1387 [SSC 1336, TMC 724]. Isolated from liver of diseased hen.	Giovanni Ghielmetti	

M. avium strain 1904038568	wild-type	*Mycobacterium avium.* Clinical human patient isolate	Alexandra Aubry	unpublished
M. avium Vet. Isolate 20-935 /2	wild-type	*Mycobacterium avium* supsp. *hominissuis.* Isolated from pig liver.	Giovanni Ghielmetti	unpublished
Endophyte MS5	wild-type	Isolated from sugar beets.	NIOO-KNAW	Carrion *et al.*, 2019
Endophyte R2A12	wild-type	Isolated from sugar beets.	NIOO-KNAW	Carrion *et al.*, 2019
Endophyte SBRA8	wild-type	Isolated from sugar beets.	NIOO-KNAW	Carrion *et al.*, 2019

846

847 **Table S2.** Imaging settings used with Zeiss LSM 900 confocal microscope.

Fluorescent protein, probe or metabolic label	Excitation (nm)	Emission (nm)
mCherry	561	570-700
SYTO 9	488	490-600
SynapseRed	488	600-700

848

849 **Table S3.** Pearson chi-square tests on flow cytometry data of *M. smegmatis* grown

850 under different conditions and exposed to TX-100. Tests are performed on averages

851 of biological triplicates and technical duplicates.

852 Separate populations: df = 2

853 Total populations: df = 4

854 *p*-values less than 0.05 are considered significant

Media	Population	Pearson chi-squared test	
		X^2	*p-value*
MB7H9	Walled (Q2)	0.01	0.99
	CWD (Q3)	0.16	0.92
	Rest (Q1 & 4)	0.01	0.99
	Total	0.18	0.99
LPB 0.6 M sucrose	Walled (Q2)	0.02	0.99
	CWD (Q3)	0.08	0.96
	Rest (Q1 & 4)	0.25	0.88
	Total	0,35	0.98
LPB 1.0 M sucrose	Walled (Q2)	0.63	0.73
	CWD (Q3)	25.15	$3.45e^{-06}$
	Rest (Q1 & 4)	26.78	$1.53e^{-06}$
	Total	52.56	$1.05e^{-10}$
Lysozyme solution	Walled (Q2)	42.69	$5.36e^{-10}$
	CWD (Q3)	26.73	$1.57e^{-06}$
	Rest (Q1 & 4)	462	$4.7e^{-101}$
	Total	531	$1.1e^{-113}$

855

856

31

857 **Table S4.** Paired student t-tests on viability assessment through CFU counting of *M.*

858 *smegmatis* grown in different conditions and exposed to TX-100. Performed on

859 biological triplicates and technical duplicates.

860 Tails = 2

861 *p*-values less than 0.05 are considered significant

		Paired student t-test		
Media	**Condition**	**CFU average**	**Standard deviation**	***p-value***
MB7H9	Control	1.82E+09	6,05E+08	
	TX-100	2.53E+09	1,39E+09	0.36
LPB 0.6 M sucrose	Control	2.62E+08	1,19E+08	
	TX-100	1.63E+08	8,94E+07	0.20
LPB 1.0 M sucrose	Control	1.87E+06	1,18E+06	
	TX-100	2.97E+04	1,21E+04	0.012
Lysozyme solution	Control	2.84E+06	2,29E+06	
	TX-100	2.49E+03	6,20E+02	0.029

862

863 **Table S5.** Minimal Inhibitory Concentration (MIC) of antibiotics in hyperosmotic

864 media

Antibiotic	MIC (μg·mL^{-1})		
	MB7H9	LPB 0 M sucrose	LPB 0.4 M Sucrose
Isoniazid	12.2	12.2	6.1
Vancomycin	19.5	9.7	2.4
D-cycloserine	97.7	390.6	390.6

865

866

867 **Table S6.** Mycobacterial genome references used for phylogenetic analysis.

Mycobacterial strain	ATCC	Genome
Mycolicibacterium smegmatis MC2-155	ATCC 70084	NC_008596.1
Mycobacterium abscessus	ATCC 19977	NC_010397.1
Mycobacterium avium subsp. avium Vet. 1387	ATCC 25291	NZ_ACFI00000000
Mycobacterium avium 101	ATCC 700898	
Mycobacterium marinum M	ATCC BAA-535	NC_010612.1
Mycobacterium bovis AF2122-97	ATCC BAA-935	NC_002945.3
Mycobacterium bovis BCG Russia	ATCC 35740	EU442641.1
Mycobacterium bovis BCG Pasteur, 1173P2	ATCC 35734	AM408590
Mycobacterium tuberculosis H37Rv	ATCC 27294	NC_000962.3
Mycobacterium ulcerans JKD8049		NZ_CP085200.1
Mycobacterium leprae TN		AL450380.2
Mycobacterium lepromatosis Mx1-22A		JRPY01000041.1
Mycobacterium sp. MS5		
Mycobacterium sp. R2A12		
Mycobacterium sp. SBRA8		

868

34

869 **Table S7.** Osmolality measurements and osmotic pressure calculations on

870 cultivation media supplemented with increasing concentrations of sucrose.

871 Δosm = osmolal gap between measured osmolality and calculated osmolarity,

872 π = osmotic pressure

Medium	Sucrose (M)	Osmolality (mOsm·kg^{-1})	Δosm (mOsm·kg^{-1})	π (mmHg)
MB7H9 [*]	Original	151.0 ± 1.3	-	2914 ± 24
LPB [**]	Original	1282.5 ± 8.3	-	24752 ± 160
MB7H9 [**]	0	144.7 ± 1.0	-	2792 ± 20
	0.1	249.8 ± 0.4	5.2	4822 ± 8
	0.2	348.3 ± 1.2	3.7	6723 ± 23
	0.4	649.8 ± 5.1	105.2	12542 ± 99
	0.6	1062.2 ± 8.4	317.5	20500 ± 162
	0.8	1252.3 ± 55.5	307.7	24170 ± 1071
	1.0	1693.7 ± 41.3	549.0	32688 ± 798
	1.2	1979.0 ± 92.1	634.3	38195 ± 1778
LPB [**]	0	229.8 ± 7.5	-	4435 ± 145
	0.1	336.0 ± 8.9	6.2	6485 ± 17
	0.2	459.5 ± 16.4	29.7	8868 ± 317
	0.4	754.2 ± 9.7	124.3	14555 ±187
	0.6	1182.5 ± 29.6	352.7	22822 ± 571
	0.8	1335.0 ± 29.7	305.2	25766 ±574
	1.0	1790.7 ± 58.1	560.8	34560 ± 1122
	1.2	2099.7 ± 55.7	669.8	40524 ± 1075

873 [*] Kept 4 °C, [**] Kept RT

874

REFERENCES

1. Allan, E. J., Hoischen, C. & Gumpert, J. Chapter 1 Bacterial L-Forms. *Advances in Applied Microbiology* **68**, 1–39 (2009).

2. Almenoff, P. L., Johnson, A., Lesser, M. & Mattman, L. H. Growth of acid fast L forms from the blood of patients with sarcoidosis. *Thorax* **51**, 530–533 (1996).

3. Banerjee, A. *et al.* Ir.iuoira. *Science (80-.).* **263**, (1994).

4. Barry, C. E. *et al.* The spectrum of latent tuberculosis: rethinking the biology and intervention strategies. *Nat. Rev. Microbiol.* **7**, 845–55 (2009).

5. Bouso, J. M. & Planet, P. J. Complete nontuberculous mycobacteria whole genomes using an optimized DNA extraction protocol for long-read sequencing. *BMC Genomics* **20**, 793 (2019).

6. Brosch, R. *et al.* Genome plasticity of BCG and impact on vaccine efficacy. *PNAS* 1–6 (2007).

7. Carrión, V. J. *et al.* Pathogen-induced activation of disease-suppressive functions in the endophytic root microbiome. *Science (80-.).* **366**, 606–612 (2019).

8. Claessen, D. & Errington, J. Cell Wall Deficiency as a Coping Strategy for Stress. *Trends Microbiol.* **27**, 1025–1033 (2019).

9. Claessen, D. & van Wezel, G. P. Bacterial proliferation. Off the Wall. *Elife* **3**, e05427 (2014).

10. Dhar, N. & McKinney, J. D. Microbial phenotypic heterogeneity and antibiotic tolerance. *Curr. Opin. Microbiol.* **10**, 30–38 (2007).

11. Domínguez-Cuevas, P., Mercier, R., Leaver, M., Kawai, Y. & Errington, J. The rod to L-form transition of Bacillus subtilis is limited by a requirement for the protoplast to escape from the cell wall sacculus. *Mol. Microbiol.* **83**, 52–66 (2012).

12. Errington, J. Cell wall-deficient, L-form bacteria in the 21st century: a personal perspective. *Biochem. Soc. Trans.* **45**, 287–295 (2017).

13. Errington, J. L-form bacteria, cell walls and the origins of life. *Open Biol.* **3**, 120143 (2013).

14. Errington, J., Mickiewicz, K., Kawai, Y. & Wu, L. J. L-form bacteria, chronic diseases and the origins of life. *Philos. Trans. R. Soc. B Biol. Sci.* **371**, (2016).

15. Etienne, G. *et al.* The cell envelope structure and properties of Mycobacterium smegmatis mc 2 155 : is there a clue for the unique transformability of the

strain？ Printed in Great Britain. *Microbiology* 2075–2086 (2005). doi:10.1099/mic.0.27869-0

16. Gupta, R. S., Lo, B. & Son, J. Phylogenomics and comparative genomic studies robustly support division of the genus Mycobacterium into an emended genus Mycobacterium and four novel genera. *Front. Microbiol.* **9**, 1–41 (2018).

17. Gupta, S. & Rodriguez, G. M. Mycobacterial extracellular vesicles and host pathogen interactions. *Pathog. Dis.* **76**, 1–6 (2018).

18. Hoffmann, C., Leis, A., Niederweis, M., Plitzko, J. M. & Engelhardt, H. Disclosure of the mycobacterial outer membrane : Cryo-electron tomography and vitreous sections reveal the lipid bilayer structure. *Proc. Natl. Acad. Sci. U. S. A.* **105**, 3963–3967 (2008).

19. Howell, M. & Brown, P. J. Building the bacterial cell wall at the pole. *Curr. Opin. Microbiol.* **34**, 53–59 (2016).

20. Hwang, T. J. *et al.* Safety of cycloserine and terizidone for the treatment of drug-resistant tuberculosis: A meta-analysis. *Int. J. Tuberc. Lung Dis.* **17**, 1257–1266 (2013).

21. Johansen, M. D., Herrmann, J. L. & Kremer, L. Non-tuberculous mycobacteria and the rise of Mycobacterium abscessus. *Nat. Rev. Microbiol.* **18**, 392–407 (2020).

22. Källenius, G., Correia-Neves, M., Buteme, H., Hamasur, B. & Svenson, S. B. Lipoarabinomannan, and its related glycolipids, induce divergent and opposing immune responses to Mycobacterium tuberculosis depending on structural diversity and experimental variations. *Tuberculosis* **96**, 120–130 (2016).

23. Kapteijn, R. *et al.* Endocytosis-like DNA uptake by cell wall-deficient bacteria. *Nat. Commun.* **13**, (2022).

24. Kawai, Y. *et al.* Cell growth of wall-free L-form bacteria is limited by oxidative damage. *Curr. Biol.* **25**, 1613–8 (2015).

25. Kawai, Y., Mickiewicz, K. & Errington, J. Lysozyme Counteracts β-Lactam Antibiotics by Promoting the Emergence of L-Form Bacteria. *Cell* **172**, 1038-1049.e10 (2018).

26. Kieser, T. *PracticalStreptomycesGenetics handbook.pdf*. (2000).

27. Kinyoun, J. J. a Note on Uhlenhuths Method for Sputum Examination, for Tubercle Bacilli. *Am. J. Public Health* **5**, 867–870 (1915).

28. Klieneberger, E. The natural occurrence of pleuropneumonia-like organisms in apparent symbiosis with Streptobacillus moniliformis and other bacteria. *J. Pathol. Bacteriol.* **40**, 93–105 (1935).

29. Lazenby, J. J., Li, E. S. & Whitchurch, C. B. Cell wall deficiency – an alternate bacterial lifestyle? *Microbiology* **168**, 001218 (2022).

30. Letunic, I. & Bork, P. Interactive Tree Of Life (iTOL): An online tool for phylogenetic tree display and annotation. *Bioinformatics* **23**, 127–128 (2007).

31. Levin-Reisman, I. *et al.* Antibiotic tolerance facilitates the evolution of resistance. *Science (80-.).* **355**, 826–830 (2017).

32. Manina, G., Dhar, N. & McKinney, J. D. Stress and host immunity amplify mycobacterium tuberculosis phenotypic heterogeneity and induce nongrowing metabolically active forms. *Cell Host Microbe* **17**, 32–46 (2015).

33. Markova, N. Cell Wall Deficiency in Mycobacteria: Latency and Persistence In Understanding tuberculosis - deciphering the secret life of the bacilli. *P.J. Cardona, ed.* 193–216 (2012). doi:10.5772/intechopen.73047

34. Mattei, B., Lira, R. B., Perez, K. R. & Riske, K. A. Membrane permeabilization induced by Triton X-100: The role of membrane phase state and edge tension. *Chem. Phys. Lipids* **202**, 28–37 (2017).

35. Mattman, L. H. Cell Wall-Deficient Forms of Mycobacteria. *Ann. New York Acad. Sci.* **174**, 852–861 (1970).

36. Mercier, R., Kawai, Y. & Errington, J. General principles for the formation and proliferation of a wall-free (L-form) state in bacteria. *Elife* **3**, e04629 (2014).

37. Mickiewicz, K. M. *et al.* Possible role of L-form switching in recurrent urinary tract infection. *Nat. Commun.* **10**, 1–9 (2019).

38. Neelsen, F. Ein casuistischer Beitrag zur Lehre von der Tuberkulose. *Cent. fiir die Med. Wissenschaften* **28**, 497 (1883).

39. Oettinger, T., Jørgensen, M., Ladefoged, A., Hasløv, K. & Andersen, P. Development of the Mycobacterium bovis BCG vaccine: Review of the historical and biochemical evidence for a genealogioal tree. *Tuber. Lung Dis.* **79**, 243–250 (1999).

40. Pankhurst, L. J. *et al.* Rapid, comprehensive, and affordable mycobacterial diagnosis with whole-genome sequencing: A prospective study. *Lancet Respir. Med.* **4**, 49–58 (2016).

41. Pfyffer, G. E. *et al.* Comparison of the mycobacteria growth indicator tube (MGIT) with radiometric and solid culture for recovery of acid-fast bacilli. *J. Clin. Microbiol.* **35**, 364–368 (1997).

42. Prados-Rosales, R. *et al.* Mycobacteria release active membrane vesicles that modulate immune responses in a TLR2-dependent manner in mice. *J. Clin. Invest.* **121**, 1471–1483 (2011).

43. Prados-Rosales, R. *et al.* Role for mycobacterium tuberculosis membrane vesicles in iron acquisition. *J. Bacteriol.* **196**, 1250–1256 (2014).

44. Ramakrishnan, L. & Falkow, S. Mycobacterium marinum persists in cultured mammalian cells in a temperature-restricted fashion. *Infect. Immun.* **62**, 3222–3229 (1994).

45. Ramijan, K. *et al.* Stress-induced formation of cell wall-deficient cells in filamentous actinomycetes. *Nat. Commun.* **9**, 5164 (2018).

46. Rasouli, M. Basic concepts and practical equations on osmolality: Biochemical approach. *Clin. Biochem.* **49**, 936–941 (2016).

47. Ratnam, S. & Chandrasekhar, S. The pathogenicity of spheroplasts of Mycobacterium tuberculosis. *Am. Rev. Respir. Dis.* **114**, 549–554 (1976).

48. Sani, M. *et al.* Direct visualization by Cryo-EM of the mycobacterial capsular layer: A labile structure containing ESX-1-secreted proteins. *PLoS Pathog.* **6**, e1000794 (2010).

49. Saxena, S., Spaink, H. P. & Forn-Cuní, G. Drug resistance in nontuberculous mycobacteria: Mechanisms and models. *Biology (Basel).* **10**, 1–22 (2021).

50. Schindelin, J. *et al.* Fiji: An open-source platform for biological-image analysis. *Nat. Methods* **9**, 676–682 (2012).

51. Segata, N., Börnigen, D., Morgan, X. C. & Huttenhower, C. PhyloPhlAn is a new method for improved phylogenetic and taxonomic placement of microbes. *Nat. Commun.* **4**, (2013).

52. Shleeva, M. O. *et al.* Dormant ovoid cells of Mycobacterium tuberculosis are formed in response to gradual external acidification. *Tuberculosis* **91**, 146–154 (2011).

53. Simmons, J. D. *et al.* Immunological mechanisms of human resistance to persistent Mycobacterium tuberculosis infection. *Nat. Rev. Immunol.* **18**, 575–589 (2018).

54. Slavchev, G., Michailova, L. & Markova, N. L-form transformation phenomenon in Mycobacterium tuberculosis associated with drug tolerance to ethambutol. *Int. J. Mycobacteriology* **5**, 454–459 (2016).

55. Snapper, S. B., Melton, R. E. & Kieser, S. M. T. Isolation and characterization of efficient plasmid transformation mutants of Mycobacterium smegmatis. *Mol. Microbiol.* **4**, 1911–1919 (1990).

56. Sohlenkamp, C. & Geiger, O. Bacterial membrane lipids: Diversity in structures and pathways. *FEMS Microbiol. Rev.* **40**, 133–159 (2015).

57. Udou, T., Ogawa, M. & Mizuguchi, Y. Spheroplast formation of Mycobacterium smegmatis and morphological aspects of their reversion to the bacillary form. *J. Bacteriol.* **151**, 1035–1039 (1982).

58. Velayati, A. A. *et al.* Populations of latent Mycobacterium tuberculosis lack a cell wall: Isolation, visualization, and whole-genome characterization. *Int. J. Mycobacteriology* **5**, 66–73 (2016).

59. Vollmer, W., Blanot, D. & De Pedro, M. a. Peptidoglycan structure and architecture. *FEMS Microbiol. Rev.* **32**, 149–167 (2008).

60. Votintseva, A. A. *et al.* Same-day diagnostic and surveillance data for tuberculosis via whole-genome sequencing of direct respiratory samples. *J. Clin. Microbiol.* **55**, 1285–1298 (2017).

61. Woo, P. C. Y., To, A. P. C., Lau, S. K. P. & Yuen, K. Y. Facilitation of horizontal transfer of antimicrobial resistance by transformation of antibiotic-induced cell-wall-deficient bacteria. *Med. Hypotheses* **61**, 503–508 (2003).

62. World Health Organization (WHO). *Global tuberculosis report 2021*. *Geneva: World Health Organisation* (2021).

63. World Health Organization (WHO). Global leprosy (Hansen disease) update, 2020: impact of COVID-19 on global leprosy control. *Wkly. Epidemiol. Rec.* **96**, 421–444 (2021).

64. World Health Organization, (WHO). *Consolidated Guidelines on Tuberculosis Treatment*. *Who* (2020).

65. Yu, J. *et al.* Both phthiocerol dimycocerosates and phenolic glycolipids are required for virulence of Mycobacterium marinum. *Infect. Immun.* **80**, 1381–1389 (2012).

66. Ziehl, F. Zur Farbung des Tuberkelbaclilus. *Dtsch. Medizinische Wochenschrif* 451 (1882).

FIGURE 1

A. MB7H10 / Standard / Stereo / 50 mm / PC / 10 µm / Hyperosmotic / LPMA

B. MB7H10 / DIC / LPMA / LPB / SYTO-9 / 10 µm

C. pCHERRY10 / BF / mCherry / SYTO 9 / 2 µm

D. LPB / BF / Day 1 / SynapseRed / 5 µm / Day 10

E. LPB / 00:00 / 5 µm / 03:10 * / 03:15 / 03:20 / 16:00

F. LPB sucrose (M) / 0 / 10 µm / 0.4 / 0.6 / 0.8 / 1:0

G. OD$_{600nm}$ (AU) / Sucrose in LPB (M) / OD$_{600nm}$ / CWD (%) / Population percentage (%)

H. M. smegmatis / mc²155 / ATCC 607 / SynapseRed / SYTO 9 / 2 µm / M. avium / MAC101 ATCC 700898 / Clinical Isolate 1904038568
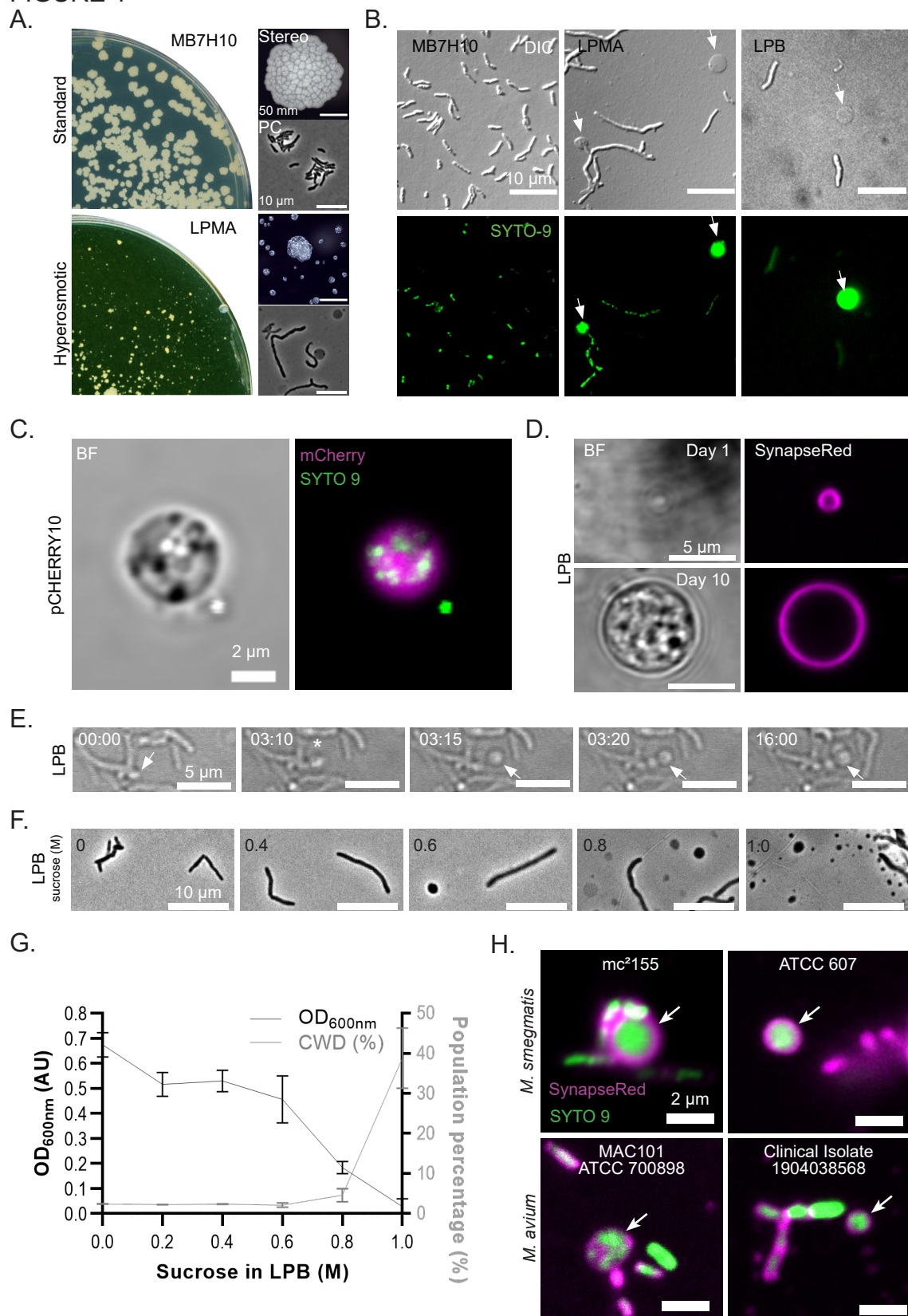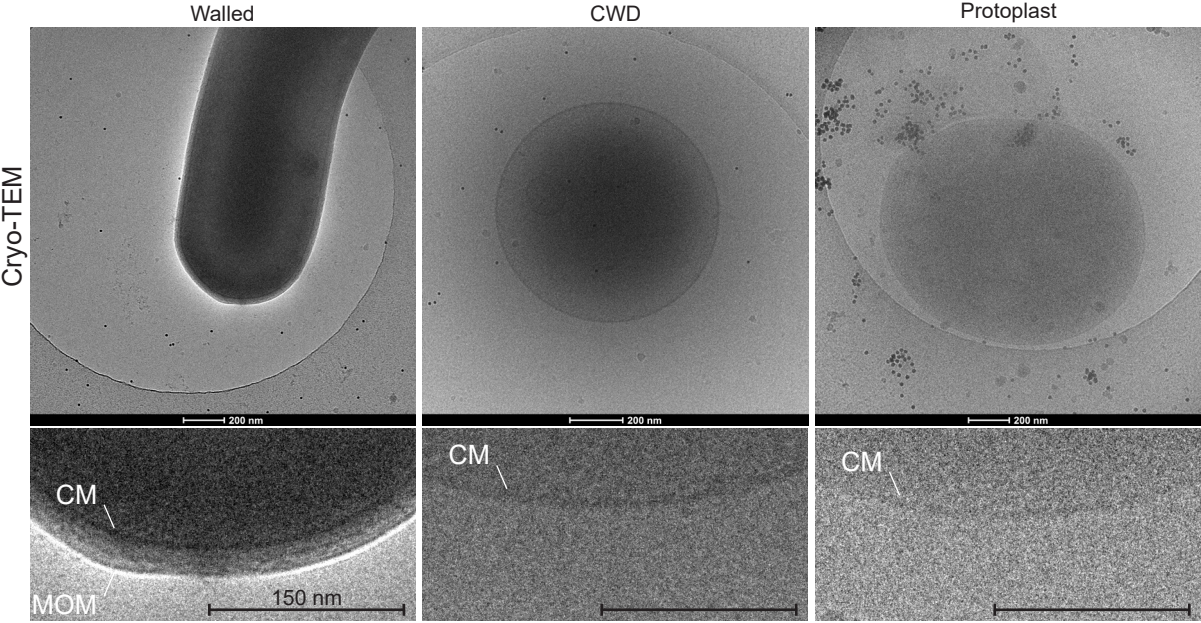
Figure 1. Hyperosmotic stress causes cell wall-deficiency in mycobacteria.
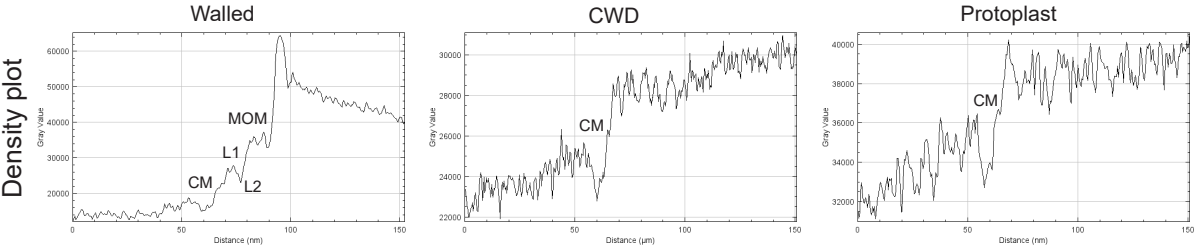
A) Plate scans, stereo images and phase contrast micrographs of M. *smegmatis* mc^{2}155 colonies grown for 3 days on standard cultivation medium MB7H10 or for 6 days on hyperosmotic LPMA medium. Scale bar represents 50 mm and 10 µm. **B)** DIC and fluorescent micrographs of *M. smegmatis* mc^{2}155 grown for 3 days on MB7H10 and LPMA plates and in liquid LPB medium. Nucleic acids were labeled with SYTO 9 for 15 min. Scale bars represent 10 µm. **C)** Confocal image of a nucleic acid-containing cell of *M. smegmatis* mc^{2}155 fluorescently labeled with pCHERRY10 (Caroll et al., 2010) after 10 days of growth in LPB medium. Nucleic acids were labeled with SYTO 9 for 15 min. Scale bar represents 2 µm. **D)** Confocal images of *M. smegmatis* mc^{2}155 cells with different diameters, 1.8 µm and 6.8 µm, respectively, formed in LPB medium. Membranes were labeled with SynapseRed for 15 min. Scale bars represent 5 µm. **E)** Stills of *M. smegmatis* mc^{2}155 showing extrusion of CWD cells in LPB medium. Scale bars represent 5 µm. **F)** Phase contrast micrographs of *M. smegmatis* mc^{2}155::pCHERRY10 grown in ascending concentrations of sucrose for 1 day. Scale bars represent 10 µm. **G)** Correlation between optical density and the number of CWD cells of *M. smegmatis* mc^{2}155::pCHERRY10 in LPB supplemented with ascending concentrations of sucrose. The number of CWD cells is represented as the percentage of all cells in the cultures, which was quantified using flow cytometry (See Figs. S1E and S2). Optical densitymeasurements (OD$_{600nm}$) was were performed over time as shown in Supplemental Figure S1F.**H)** Confocal images of mycobacterial strains grown in LPB supplemented with 1.0 M sucrose.Images were made after 2 days (*M. smegmatis* strains) or 2 weeks (*Mycobacterium avium* complex(MAC) strains). Nucleic acids and cell membrane were labeled with SYTO 9 and SynapseRed,respectively, for 15 min. Scale bars represent 2 µm.
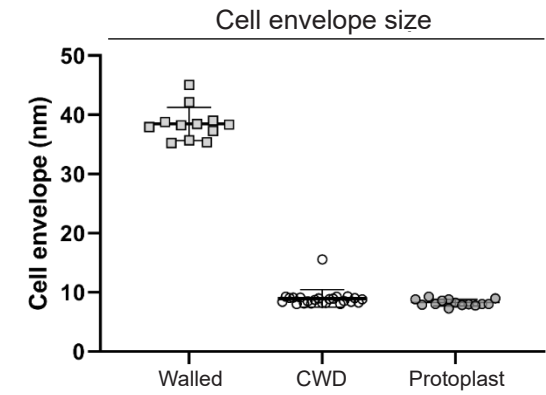
FIGURE 2
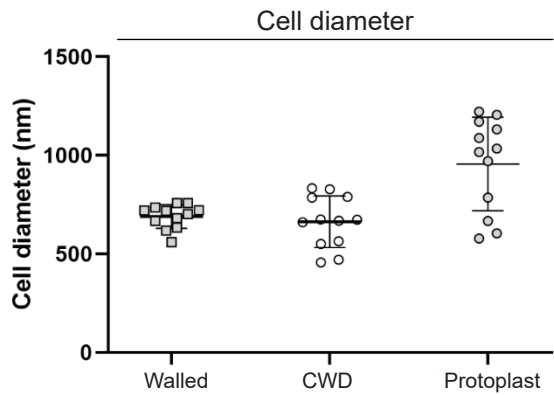
A.

B.

C.

D.

Figure 2. Wall-deficient cells of *M. smegmatis* lack major cell wall components.
A) Cryo-Transmission Electron Microscopy (TEM) images of walled cells, CWD cells or protoplasts of *M. smegmatis* mc^{2}155. Walled cells were grown in MB7H9 liquid medium and blotted directly from culture. CWD cells were enriched after 8 days of growth in LPB 1.0 M sucrose. Protoplasts were generated by lysozyme treatment in P-buffer through an adjusted mycobacterial protoplast protocol (see Material and Methods). Scale bars represent 200 nm. The lower panels represent zoomed in areas and scale bars correspond to 150 nm. CM, cytoplasmic membrane; MOM, mycobacterial outer membrane (Sani et al., 2010). **B)** Gray scale density plot measurements from zoomed-in Cryo-TEM micrographs across the cell envelope in right-angle (90°). CM, cytoplasmic membrane; L1 and L2, domain-rich periplasmic layers; MOM, mycobacterial outer membrane (Hoffmann et al., 2008). **C)** Cell envelope measurements based on density plots of selected cells (n = 6). Measurements were performed in duplicate at different locations per cell. The envelope diameter of CWD cells and protoplasts were measured in duplicate per cell (in 90° angle) and the walled cells were measured at the tip and at the side wall in relative distance from the tip curvature. **D)** Cell diameter measurements of selected cells (n=6). The diameter was measured in duplicate per cell, in perpendicular for spherical cells (CWD cells and protoplast) and   perpendicular to the longitudinal axis of the rod shaped cell (side to side walls), with an minimum of 50 nm distance (Walled).
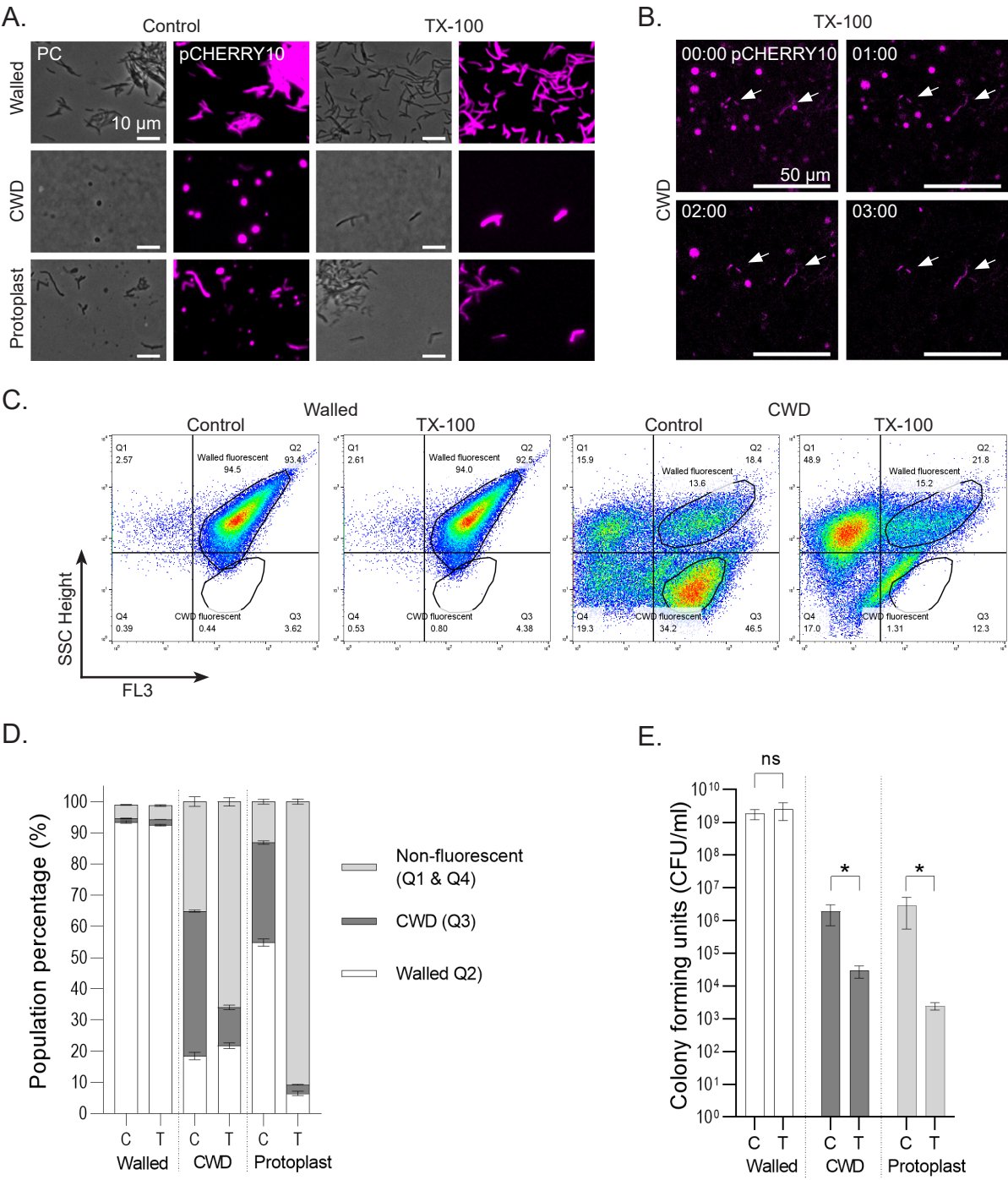
FIGURE 3

A.

Control | TX-100

Walled — PC / pCHERRY10 — 10 µm

CWD

Protoplast

B.

TX-100

CWD — 00:00 pCHERRY10 / 01:00 / 02:00 / 03:00 — 50 µm

C.

Walled — Control | TX-100
CWD — Control | TX-100

Walled Control:
Q1 2.57 | Q2 93.4 Walled fluorescent 94.5
Q4 0.39 | CWD fluorescent 0.44 | Q3 3.62

Walled TX-100:
Q1 2.61 | Q2 92.5 Walled fluorescent 94.0
Q4 0.53 | CWD fluorescent 0.80 | Q3 4.38

CWD Control:
Q1 15.9 | Q2 18.4 Walled fluorescent 13.6
Q4 19.3 | CWD fluorescent 34.2 | Q3 46.5

CWD TX-100:
Q1 48.9 | Q2 21.8 Walled fluorescent 15.2
Q4 17.0 | CWD fluorescent 1.31 | Q3 12.3

SSC Height / FL3

D.

Population percentage (%)

C T Walled | C T CWD | C T Protoplast

Non-fluorescent (Q1 & Q4)
CWD (Q3)
Walled Q2

E.

Colony forming units (CFU/ml)

C T Walled (ns) | C T CWD (*) | C T Protoplast (*)

Figure 3. Wall-deficient cells of *M. smegmatis* are viable.

A) Phase contrast and fluorescent images of M. smegmatis mc2155::pCHERRY10 walled cells, CWD cells and protoplasts after exposure to detergent 0.1% Triton X-100 (TX-100) for 15 min. As a control MQ was added to the cells. Scale bars represent 10 µm. **B)** Time-lapse images of M. smegmatis mc2155::pCHERRY10 exposed to 0.1 % TX-100. Please note that walled cells, indicated with arrows, do not disappear over time in contrast to CWD cells. Scale bars represent 50 µm. Time is indicated in hours. **C)** Flow cytometry plots of M. smegmatis mc2155::pCHERRY10 walled and CWD cells in response water (control) or t Triton X-100 exposure (TX-100) in triplicates. Plots were divided in four quadrants representing Highly complex, non-fluorescent particles (Q1), Highly complex fluorescent particles (Q2, Walled cells), Less complex, fluorescent particles (Q3, CWD cells), and Less complex, non-fluorescent particles (Q4). Please note that the CWD cells disappear when treated with TX-100 (right panels). **D)** Quantification of flow cytometry data. White bars represent walled cells, while light grey and dark grey represent non-fluorescent particles and CWD cells, respectively. Please note that the addition of TX-100 (T), in contrast to the water control (C), dramatically reduces the number of CWD cells and protoplasts, while having no effect on the walled cells. All measurements were performed in triplicate (see Fig. S6). **E)** Quantification of Colony Forming Units (CFU) counts of walled cells, CWD cells and protoplasts after the exposure to TX-100 (T) or water (C). Colonies were counted after 3 days. All measurements were performed in triplicate.
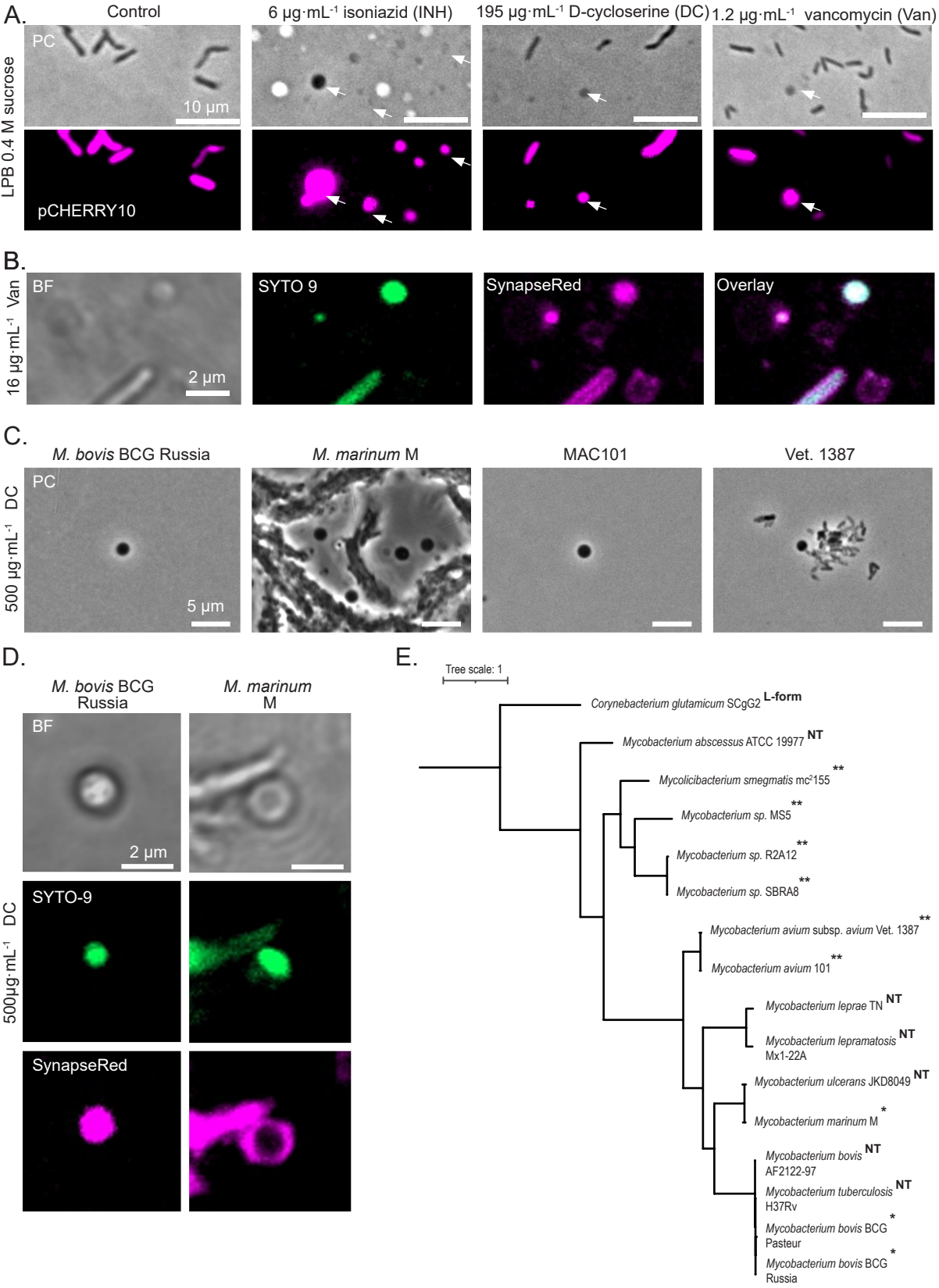
FIGURE 4

A.

Control | 6 µg·mL⁻¹ isoniazid (INH) | 195 µg·mL⁻¹ D-cycloserine (DC) | 1.2 µg·mL⁻¹ vancomycin (Van)

LPB 0.4 M sucrose

PC

10 µm

pCHERRY10

B.

16 µg·mL⁻¹ Van

BF | SYTO 9 | SynapseRed | Overlay

2 µm

C.

500 µg·mL⁻¹ DC

M. bovis BCG Russia | *M. marinum* M | MAC101 | Vet. 1387

PC

5 µm

D.

M. bovis BCG Russia | *M. marinum* M

BF

2 µm

500µg·mL⁻¹ DC

SYTO-9

SynapseRed

E.

Tree scale: 1

Corynebacterium glutamicum SCgG2 **L-form**

Mycobacterium abscessus ATCC 19977 **NT**

Mycolicibacterium smegmatis mc²155 ******

Mycobacterium sp. MS5 ******

Mycobacterium sp. R2A12 ******

Mycobacterium sp. SBRA8 ******

Mycobacterium avium subsp. *avium* Vet. 1387 ******

Mycobacterium avium 101 ******

Mycobacterium leprae TN **NT**

Mycobacterium lepramatosis Mx1-22A **NT**

Mycobacterium ulcerans JKD8049 **NT**

Mycobacterium marinum M *****

Mycobacterium bovis AF2122-97 **NT**

Mycobacterium tuberculosis H37Rv **NT**

Mycobacterium bovis BCG Pasteur *****

Mycobacterium bovis BCG Russia *****

Figure 4. Cell wall-targeting antibiotics induces wall-deficiency in mycobacteria.
A) Images of *M. smegmatis* mc2155::pCHERRY10 after 7 days of growth in the presence of 6 μg·mL^{-1} isoniazid, 195 μg·mL^{-1} D-cycloserine or 1.2 μg·mL^{-1} vancomycin. The control shows growth without the addition of antibiotics. CWD cells are indicated by arrows. Scale bars represent 10 μm. **B)** Confocal images showing CWD cells of *M. smegmatis* mc2155 formed after 5 days of growth in LPB (0.4 M sucrose) supplemented with 16 μg·mL^{-1} vancomycin. Nucleic acids and cell membranes were labeled with SYTO 9 and SynapseRed, respectively. CWD cells are indicated by arrows. Scale bars represent 5 μm. **C)** Phase contrast micrographs of *M. bovis* BCG Russia, *M. marinum* M and *M. avium* strains MAC101 and Vet. 1387 exposed to 500 μg·mL^{-1} D-cycloserine in LPB 0.4 M sucrose for 8 days. Scale bars represent 5 μm. **D)** Confocal images of DNA containing CWD cells of *M. bovis* BCG Russia and *M. marinum* M, formed after 8 days of growth in LPB (0.4 M sucrose) supplemented with 500 μg·mL^{-1} D-cycloserine. Nucleic acids and cell membranes were labeled with SYTO 9 and SynapseRed, respectively. Scale bars represent 2 μm. **E)** Phylogenetic tree of mycobacteria based on whole genome sequences. Asterisk(s) indicate strains tested in this study with the natural ability to form CWD cells in the absence (**) or in the presence (*) of antibiotics. Strains that were "not tested" are indicated with the designation NT. As outgroup *Corynebacterium* was included, which was shown to be capable of propagating as an L-form (Mercier *et al.*, 2014). Reference genomes are listed in Supplemental Table 6.
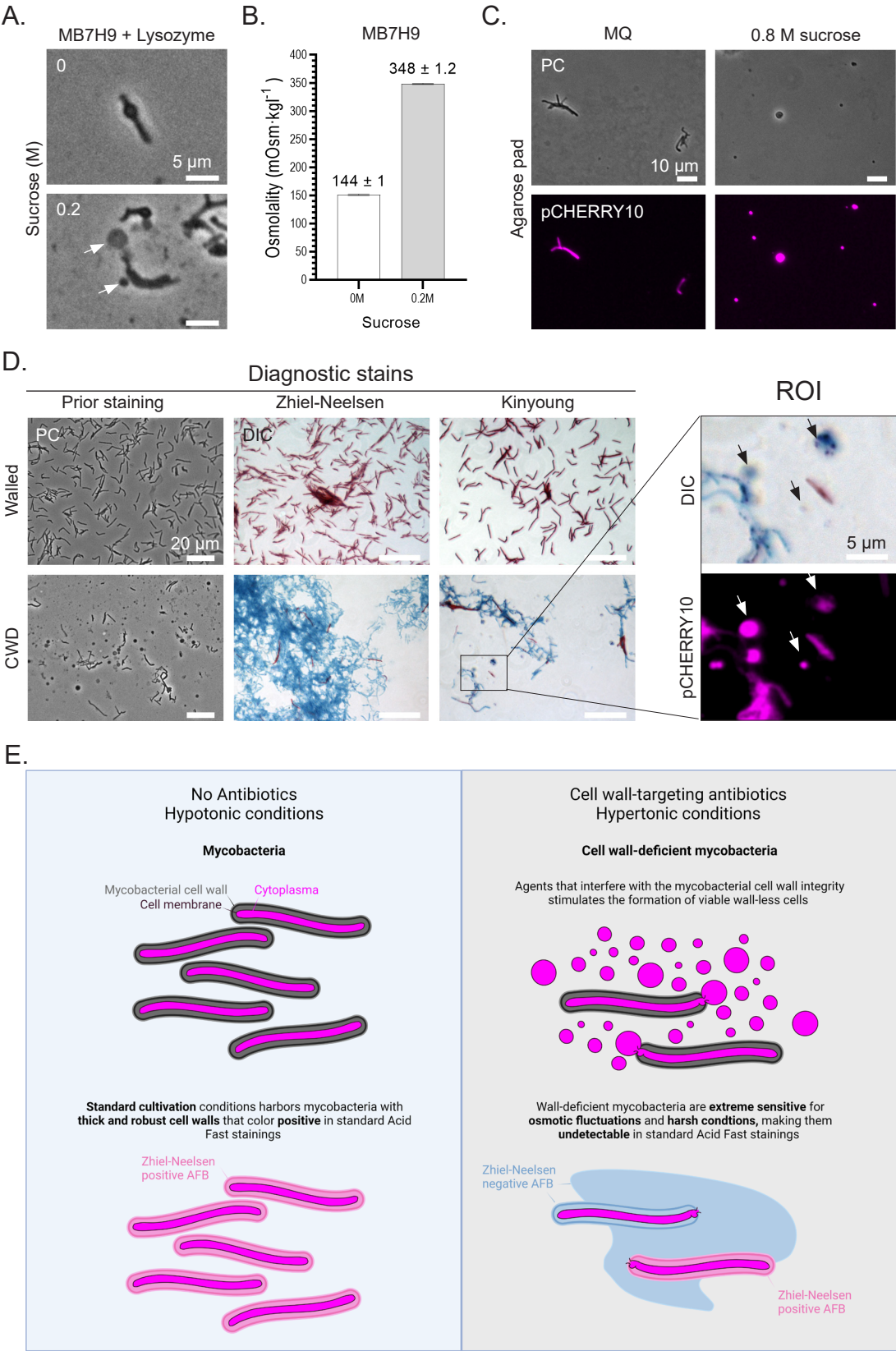
FIGURE 5

A. MB7H9 + Lysozyme

Sucrose (M): 0, 0.2

5 µm

B. MB7H9

Osmolality (mOsm·kgl⁻¹)

144 ± 1 (0M), 348 ± 1.2 (0.2M)

Sucrose

C. MQ / 0.8 M sucrose

Agarose pad — PC — 10 µm

pCHERRY10

D. Diagnostic stains

Prior staining | Zhiel-Neelsen | Kinyoung | ROI

Walled / CWD

PC / DIC — 20 µm

DIC / pCHERRY10 — 5 µm

E.

No Antibiotics
Hypotonic conditions

Mycobacteria

Mycobacterial cell wall / Cytoplasma
Cell membrane

Standard cultivation conditions harbors mycobacteria with thick and robust cell walls that color positive in standard Acid Fast stainings

Zhiel-Neelsen positive AFB

Cell wall-targeting antibiotics
Hypertonic conditions

Cell wall-deficient mycobacteria

Agents that interfere with the mycobacterial cell wall integrity stimulates the formation of viable wall-less cells

Wall-deficient mycobacteria are extreme sensitive for osmotic fluctuations and harsh condtions, making them undetectable in standard Acid Fast stainings

Zhiel-Neelsen negative AFB

Zhiel-Neelsen positive AFB

Figure 5. CWD cells of mycobacteria are undetectable by conventional diagnostics.

A) Phase contrast images of *M. smegmatis* mc^{2}155 after exposure to 1 mg·mL^{-1} lysozyme for 24 hours in MB7H9 supplemented with or without 0.2 M sucrose. The presence of CWD cells are indicated by arrows. Scale bars represent 5 μm. **B)** Osmolality measurements of MB7H9 supplemented with or without 0.2 M sucrose. Measurements were performed in sextuplicate. **C)** Images of *M. smegmatis* mc^{2}155::pCHERRY10 CWD cells formed in LPB (1.0 M sucrose) mounted on MQ and MQ/sucrose (0.8 M) agar pads. Please note that all CWD cells are absent when placed on MQ agar pads. Scale bars represent 10 μm. **D)** DIC images of conventional Ziehl-Neelsen staining and Kinyoun staining on *M. smegmatis* mc^{2}155::pCHERRY10 walled and enriched CWD cells. Acid fast bacteria (AFB) stain (positively) red, while the blue color indicates "background". Phase contrast images were taken before the staining procedure. Please note that the fluorescent (CWD) cells are visible in the region of interest (ROI), which, however, do not stain red. CWD cells are indicated by arrows. Scale bars represent 10 and 5 μm. **E)** Schematic model representing the application of Ziehl-Neelsen staining on walled and CWD mycobacteria in hypo- (left) and hypertonic (right) conditions. Please note that wall-targeting agents further stimulate the formation of CWD cells, which remain undetected by this staining method. Created with BioRender.com.

SUPPLEMENTAL FIGURE 1

Figure S1. Formation of CWD cells in *M. smegmatis* containing DNA.
A) Confocal images of nucleic acid containing CWD cells from *M. smegmatis* mc^{2}155 with relative large diameters formed overtime in LPB. Nucleic acid and membrane were labeled with SYTO 9 and SynapseRed, respectively. Scale bars represent 2 μm. **B)** Image of *M. smegmatis* mc^{2}155 walled cells and CWD cells grown for 10 days in LPB (1.0 M sucrose). Nucleic acid and membrane were labeled with SYTO 9 and SynapseRed, respectively. Scale bar represent 5 μm. **C)** Cell diameter measurements of nucleic acid containing CWD cells over time (n = 480-684 per time point, single measurement per CWD cell). Graph represents measured means and standard deviation. **D)** Confocal Z-stack images of *M. smegmatis* mc^{2}155::pCHERRY10 CWD cell grown 10 days in LPB. Nucleic acids were labeled with SYTO 9 for 15 min. Confocal images were taken in 8 times Z-stacks of 270 nm. Scale bar represents 5 μm. **E)** Quantification of flow cytometry data (see Fig. S2) of *M. smegmatis* mc^{2}155::pCHERRY10 grown for 2 days in LPB containing various concentrations of sucrose. White bars represent walled cells, while light grey and dark grey represent non-fluorescent particles and CWD cells, respectively. Please note that increasing the concentration of sucrose results in a higher number of CWD cells. **F)** Growth curve based on optical density measurements (OD$_{600nm}$) of *M. smegmatis* mc^{2}155::pCHERRY10 grown for 4 days in LPB containing various concentrations of sucrose. Please note that increasing the concentration of sucrose, results in the inhibition of growth.
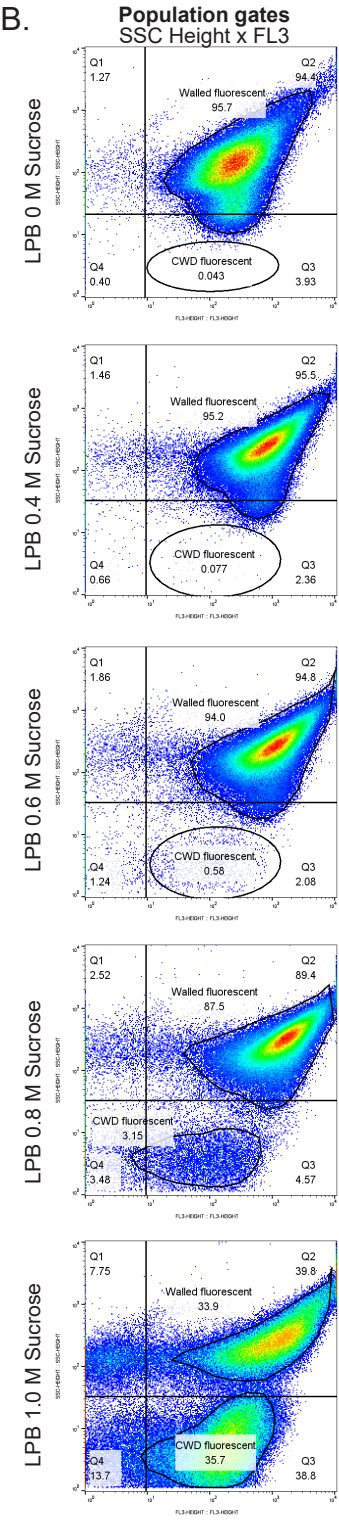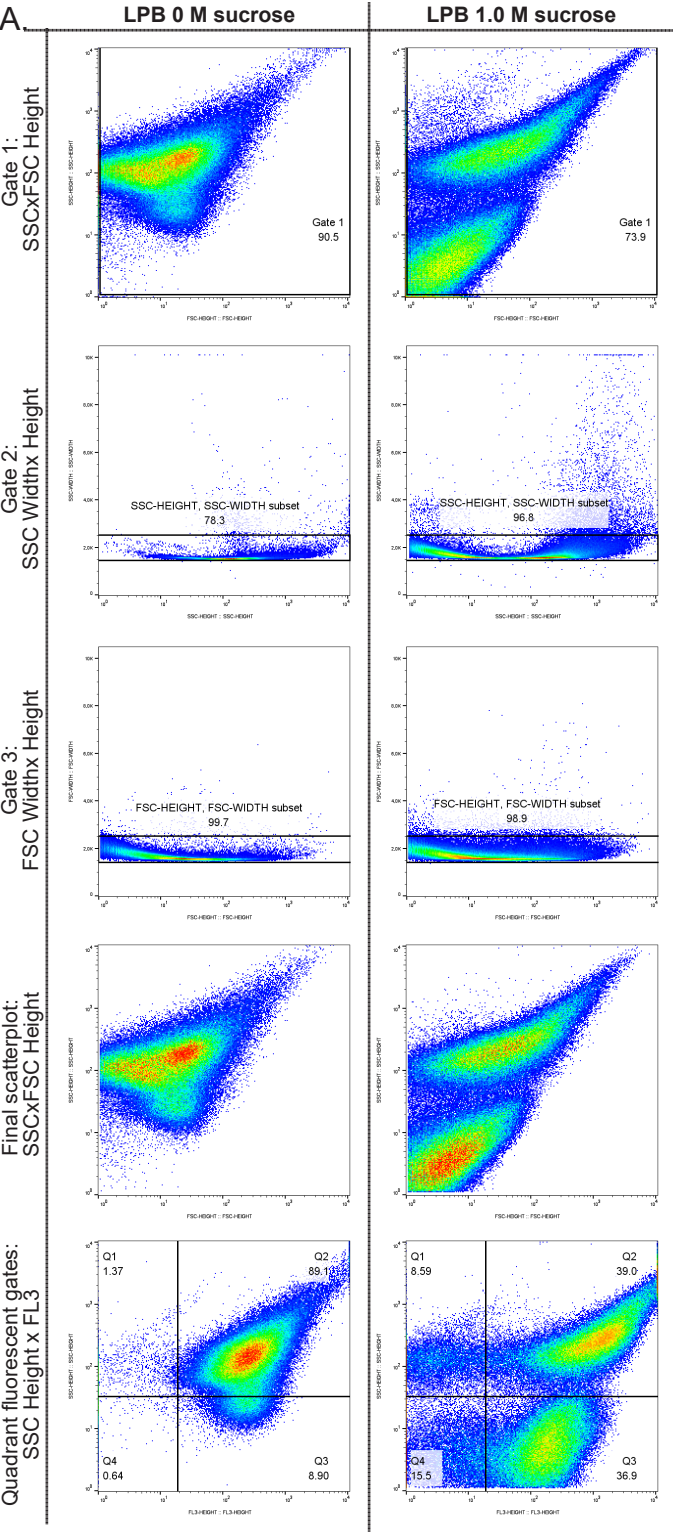
SUPPLEMENTAL FIGURE 2

Figure S2. Flow cytometry processing of fluorescent labelled walled and CWD cells of *M. smegmatis*

Flow cytometry gating workflow for remove outliers and select populations of interest. **A)** Removal of outliers represented by the two extremity conditions, LPB supplemented with 0 M and 1.0 M sucrose. Gate 1 in the FSC x SSC Height log, to remove background outliers present on both axis. Gate 2 in the SSC Height x Width log to remove outliers in the SSC. Gate 3 in the FSC Height x Width log to remove outliers in the FSC. Populations represented in SSC x fluorescent filter 3 (FL3), bandwidth 615/25 with laser 56.1 Simple iQuadrants bins gating for estimated separation of populations, namely Highly complex, non-fluorescent particles (Q1), Highly complex, fluorescent particles (Q2, Walled), Less complex, fluorescent particles(Q3, CWD cells), and Less complex, non-fluorescent particles (Q4). **B)** Specific gates drawn to specific populations of interest in SSC x FL3, including subpopulations in lower sucrose conditions of propagating walled cells with nascent, less complex, cell walls prior cell wall modifications. Relative population percentages represented by the populations "Walled fluorescent" and "CWD fluorescent".
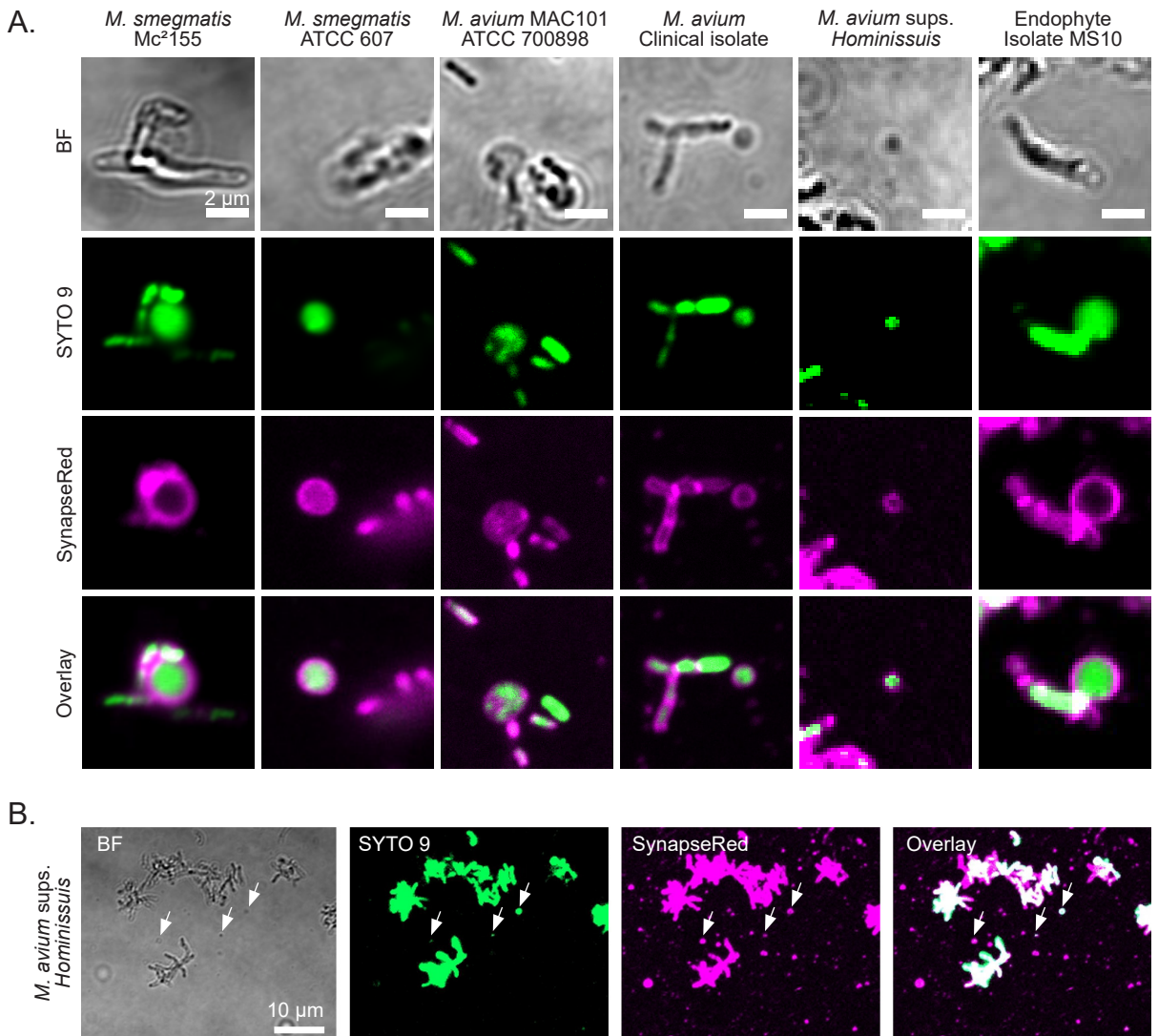
Figure S3. CWD formation in response to hyperosmotic conditions in various mycobacterial species
Confocal micrographs of various mycobacterial strains grown in LPB (1.0 M sucrose). Cells were fluorescently dyed with SYTO 9 and SynapseRed to label nucleic acids and membranes, respectively. **A)** Mycobacterial strains were grown for either 2 days (*M. smegmatis* strains) or 2 weeks (*Mycobacterium avium* complex strains) at 37 °C 100 RPM, or were grown 1 week at 30 °C 100 RPM (endophytic isolates). Scale bars represent 2 μm. **B)** Veterinary isolate *Mycobacterium avium* subsp. *hominissuis* 20-935 /2 grown for 2 weeks at 37 °C 100 RPM. Please note that this strain produces some CWD cells, but mostly empty membrane vesicles. Scale bar represent 10 μm.
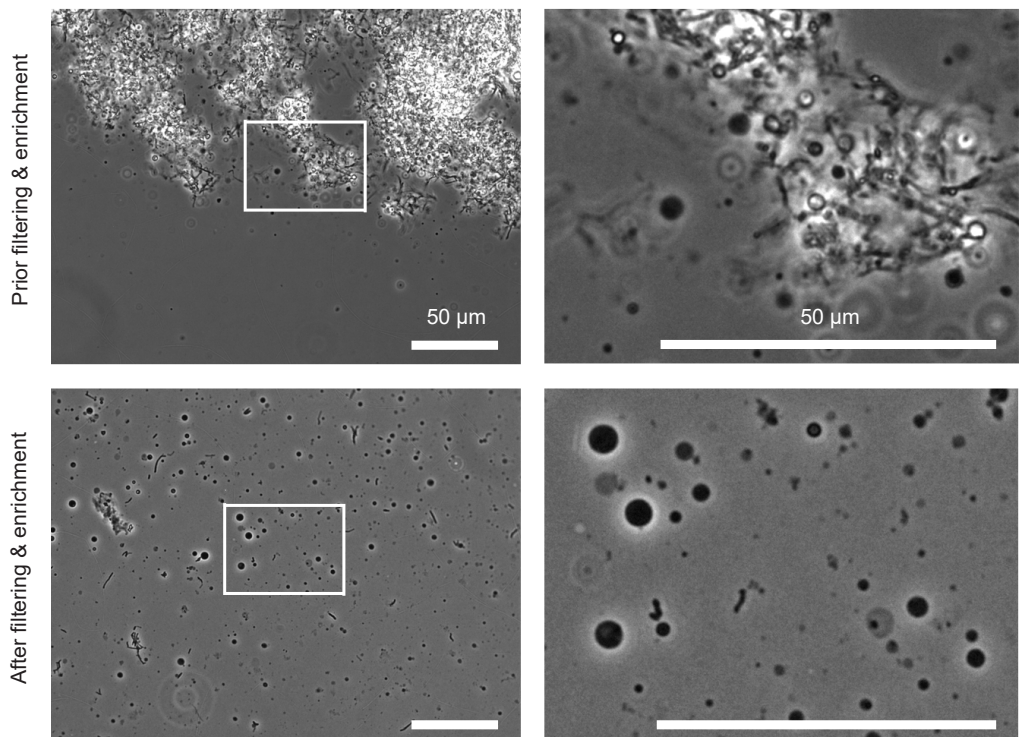
SUPPLEMENTAL FIGURE 4

a.
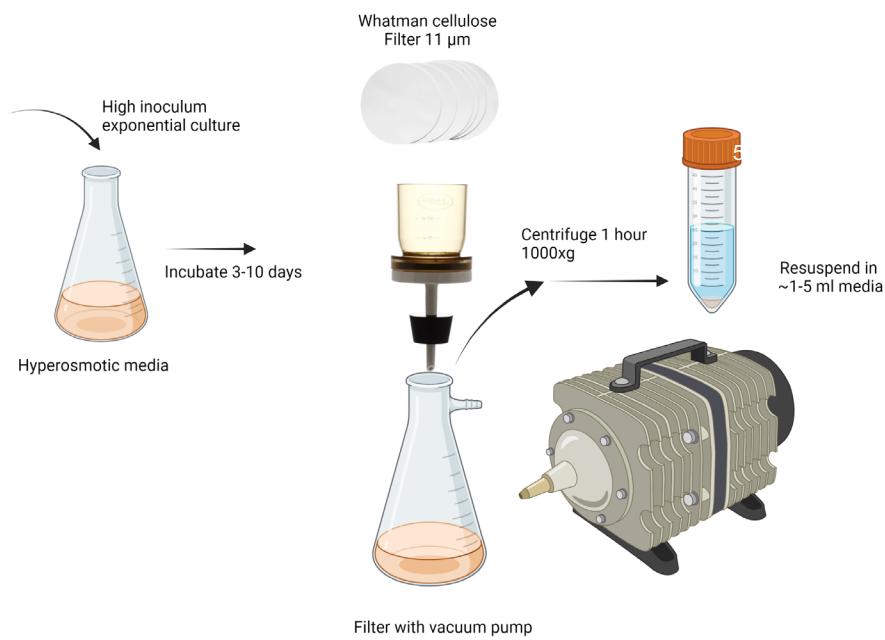
b.

Figure S4. Enrichment of mycobacterial CWD cells
A) Enrichment method of CWD cells utilizing particle retention of 11 µm and slow centrifugation. In short, CWD cells are produced in as described in Material and Methods. Incubate until CWD cells are formed and filter culture with vacuum pump. Centrifuge filtrate for 1 hour at low centrifuging force (1000 x g). Please note that low centrifuging force is needed to avoid cell shearing of the sensitive CWD cells. Resuspend loose pellet in left-over supernatant. Created with BioRender.com. **B)** Phase contrast images of M. smegmatis mc2155 CWD cells grown for 8 days in LPB (1.0 M sucrose), before and after enrichment. Scale bars represent 50 µm.
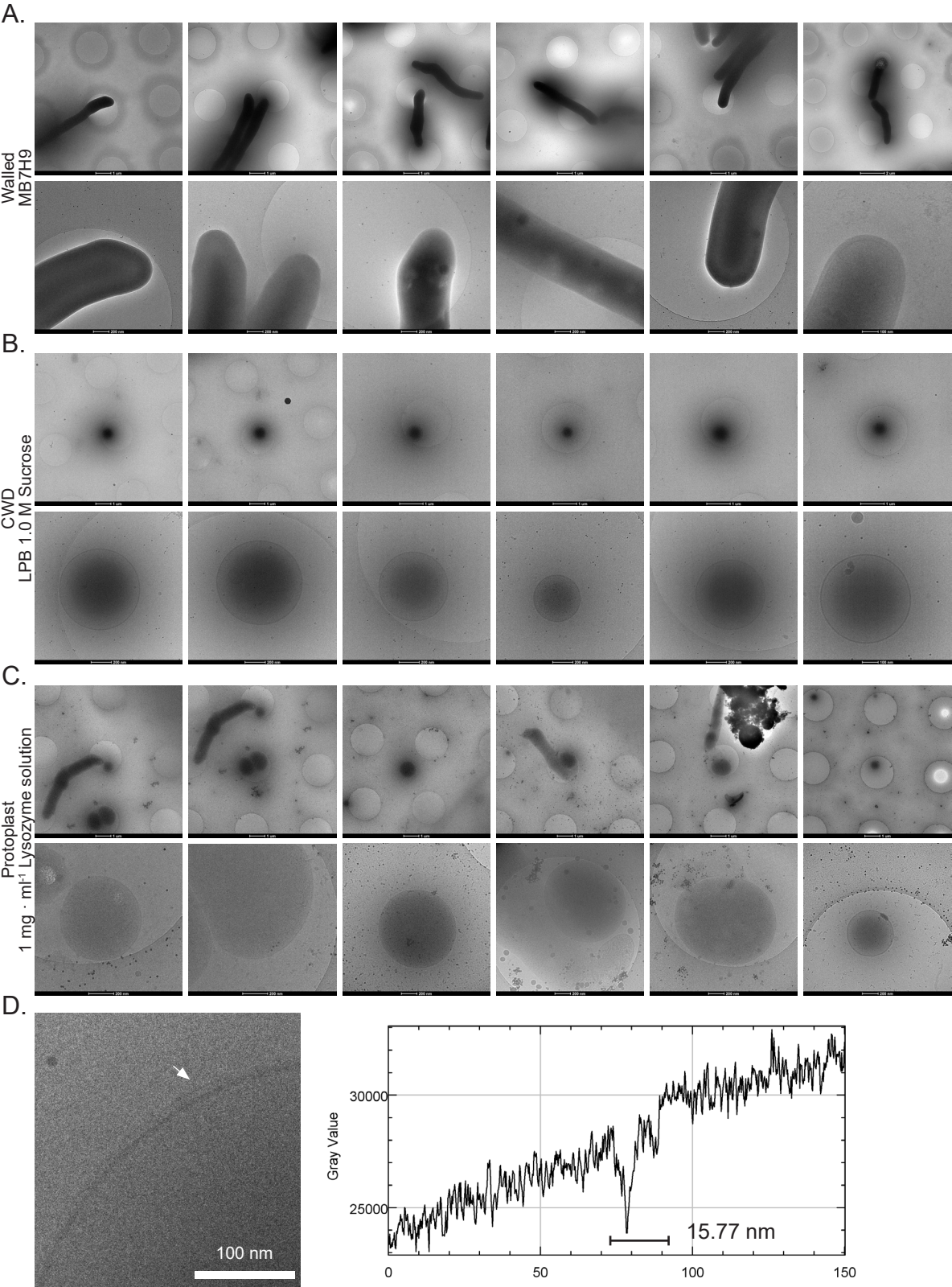
SUPPLEMENTAL FIGURE 5

A.

Walled MB7H9

B.

CWD
LPB 1.0 M Sucrose

C.

Protoplast
1 mg · ml⁻¹ Lysozyme solution

D.

100 nm

15.77 nm

Figure S5. Cryo-TEM images of various cells of M. smegmatis.
A) Cryo- TEM images of exponential-phase grown *M. smegmatis* mc^{2}155 in MB7H9 liquid media, blotted directly from culture. Selected walled cells used for analysis. Scale bars represent 1 μm, 2 μm, 200 nm or 100 nm. **B)** Cryo-TEM micrographs of *M. smegmatis* mc^{2}155 enriched CWD cells, grown 8 days in LPB 1.0 M Sucrose. Selected CWD cells used for analysis. Scale bars represents 1 μm, 200 nm or 100 nm. **C)** Cryo-TEM micrographs of *M. smegmatis* mc^{2}155 artificial produced protoplasts in P-buffer. Selected protoplasts used for analysis. Scale bars represents 1 μm or 200 nm. **D)** Cryo-TEM micrograph region of interest in shows wall-like structures detected on top of plasma membrane of *M. smegmatis* mc^{2}155 enriched CWD cell, indicated by arrow. Density plot of 150 nm across cell membrane shows an extra depth representing the wall-like structure, measuring an increase in cell-envelope size to 15.77 nm. Scale bar represents 100 nm.
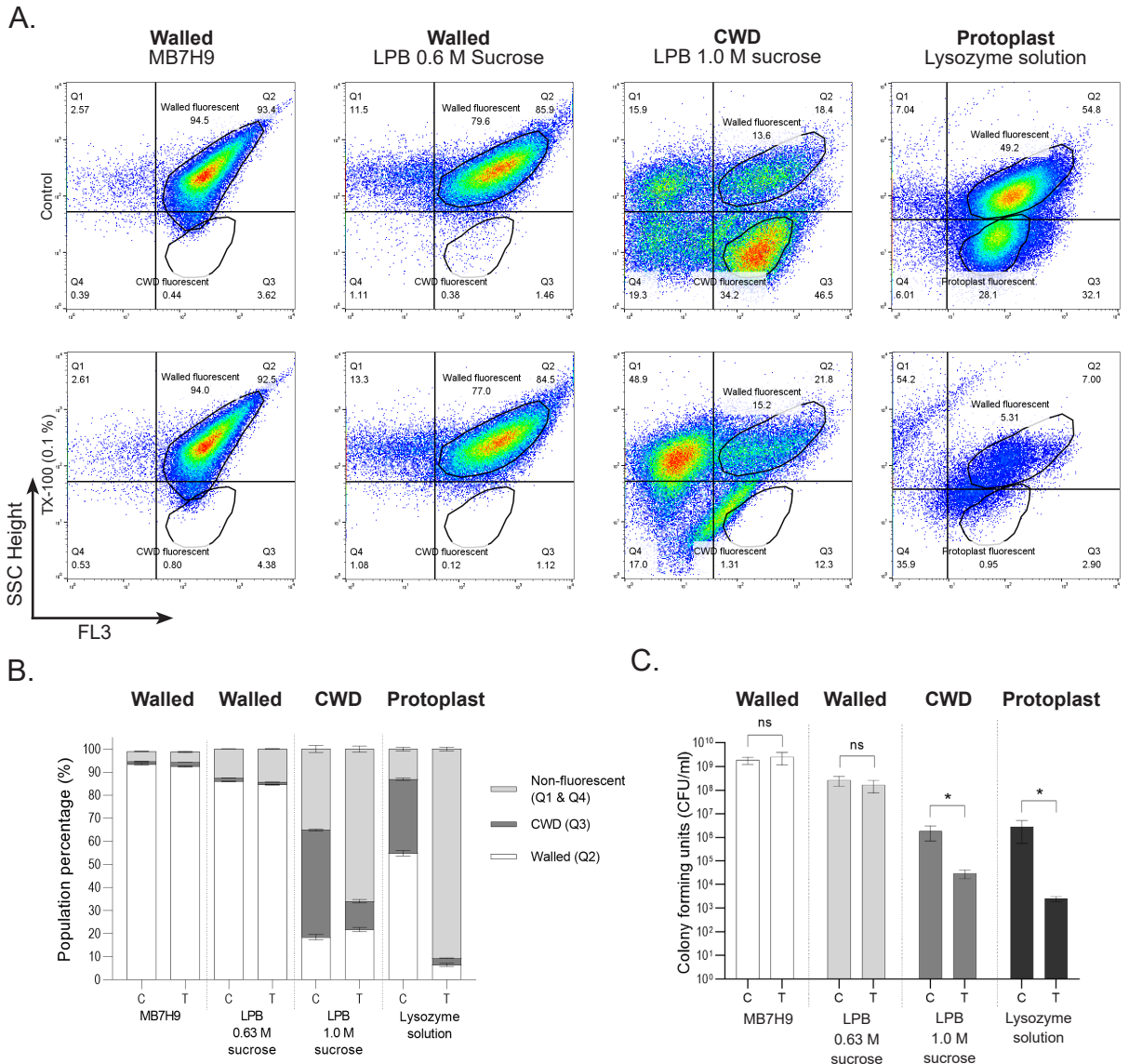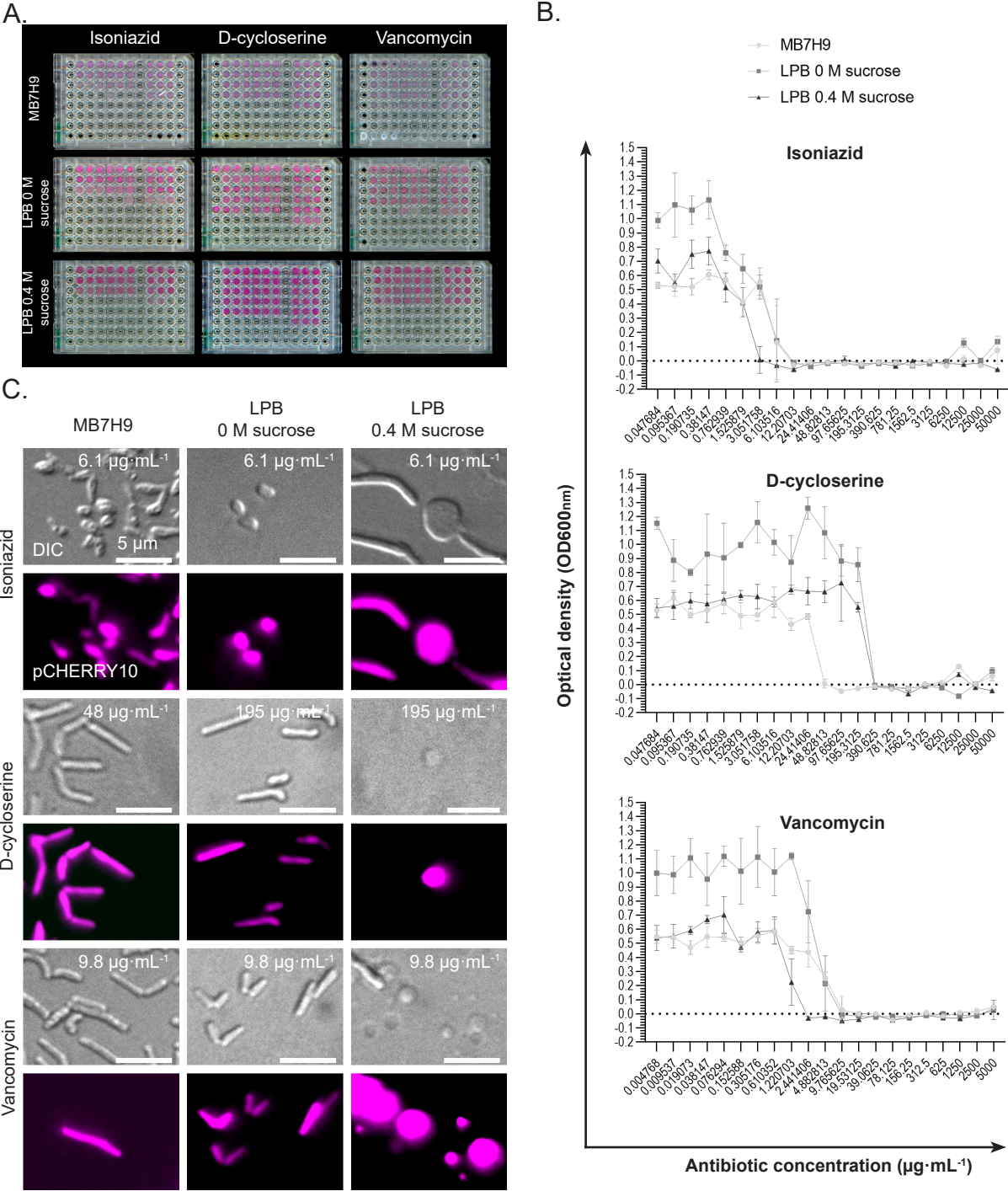
Figure S6. CWD cells are sensitive to detergent Triton X-100

A) Flow cytometry plots of *M. smegmatis* mc^{2}155::pCHERRY10 walled cells, either grown in MB7H9 or LPB (0.63 M sucrose), CWD cells, grown in LPB (1.0 M sucrose) and protoplasts (Lysozyme solution) exposed to water (control) or the detergent TX-100. Plots were divided in four quadrants representing Highly complex, non-fluorescent particles (Q1), Highly complex fluorescent particles (Q2, Walled cells), Less complex, fluorescent particles (Q3, CWD cells), and Less complex, non-fluorescent particles (Q4). Relative population percentages represented by the populations "Walled fluorescent" and "CWD fluorescent". **B)** Quantification of flow cytometry data. White bars represent walled cells, while light grey and dark grey represent non-fluorescent particles and CWD cells, respectively. Please note that the addition of TX-100 (T), in contrast to the water control (C), dramatically reduces the number of CWD cells grown in LPB (1.0 M sucrose) and protoplasts (Lysozyme solution), while having no effect on the walled cells grown in MB7H9 and LPB (0.63 M sucrose). **C)** Quantification of Colony Forming Units (CFU) counts of walled cells (MB7H9 or LPB 0.63 M sucrose), CWD cells (LPB 1.0 M sucrose) and protoplasts (Lysozyme solution) after the exposure to TX-100 (T) or water (C). Colonies were counted after 3 days. All measurements were performed in biological triplicates and technical duplicates.

Figure S7. CWD formation in MIC assays of cell wall targeting antibiotics.
MIC assays of *M. smegmatis* mc²155::pCHERRY10 in response to isoniazid, D-cycloserine and vancomyin in either MB7H9, LPB 0 M sucrose or LPB 0.4 M sucrose, performed in 96-well plates. Biological replicates were applied. Data was collected after 7 days. MIC determinations in hyperosmotic media are listed in Supplemental Table 5. **A)** Scanning images of the 96-well plates. **B)** Optical density measurements of the MIC plates. **C)** DIC-fluorescent images of walled and CWD cells. Please note that CWD cells are solely observed in sucrose supplemented LPB in response to the presence of antibiotics.
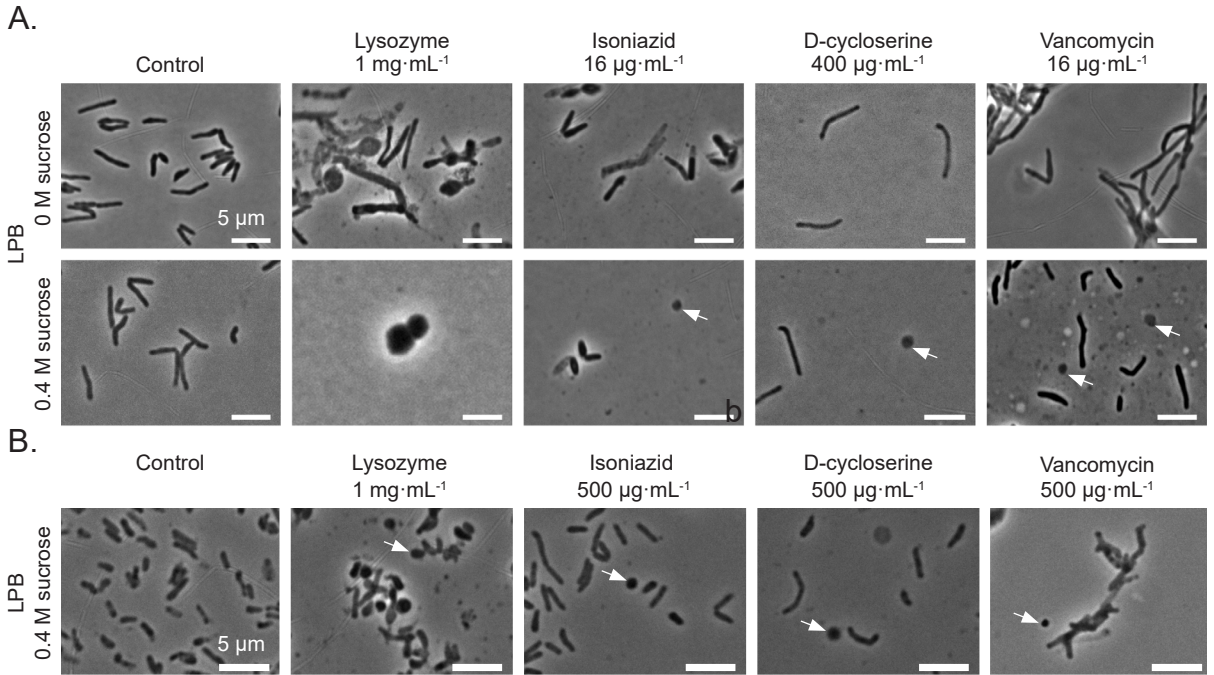
SUPPLEMENTAL FIGURE 8

A.

B.

Figure S8. Cell wall-targeting antibiotics induces the formation of CWD cells in M. smegmatis

Phase-contrast images showing CWD cells of *M. smegmatis* mc^{2}155 formed in LPB (0.4 M sucrose) in response to cell wall-targeting antibiotics. Controls includes 1 mg/mL lysozyme + 25 mM MgCl2 (positive control) and no supplementation (negative control). **A)** Formation of CWD cells after 5 days exposure to either 16 µg·mL^{-1} isoniazid, 400 µg·mL^{-1} D-cycloserine or 16 µg·mL^{-1} vancomycin. Scale bars represent 10 µm. **B)** Formation of CWD cells after 8 days exposure to elevated antibiotic concentrations, namely 500 µg·mL-1. Scale bars represent 5 µm.

SUPPLEMENTAL FIGURE 9

A. LPB 0.4 M sucrose

Control | Lysozyme 1 mg·mL⁻¹ | Isoniazid 500 µg·mL⁻¹ | D-cycloserine 500 µg·mL⁻¹ | Vancomycin 500 µg·mL⁻¹

M. avium Complex (MAC): MAC101, Vet. 1337, Clinical isolate, Vet. isolate

B. *M. bovis* BCG: Pasteur, Russia

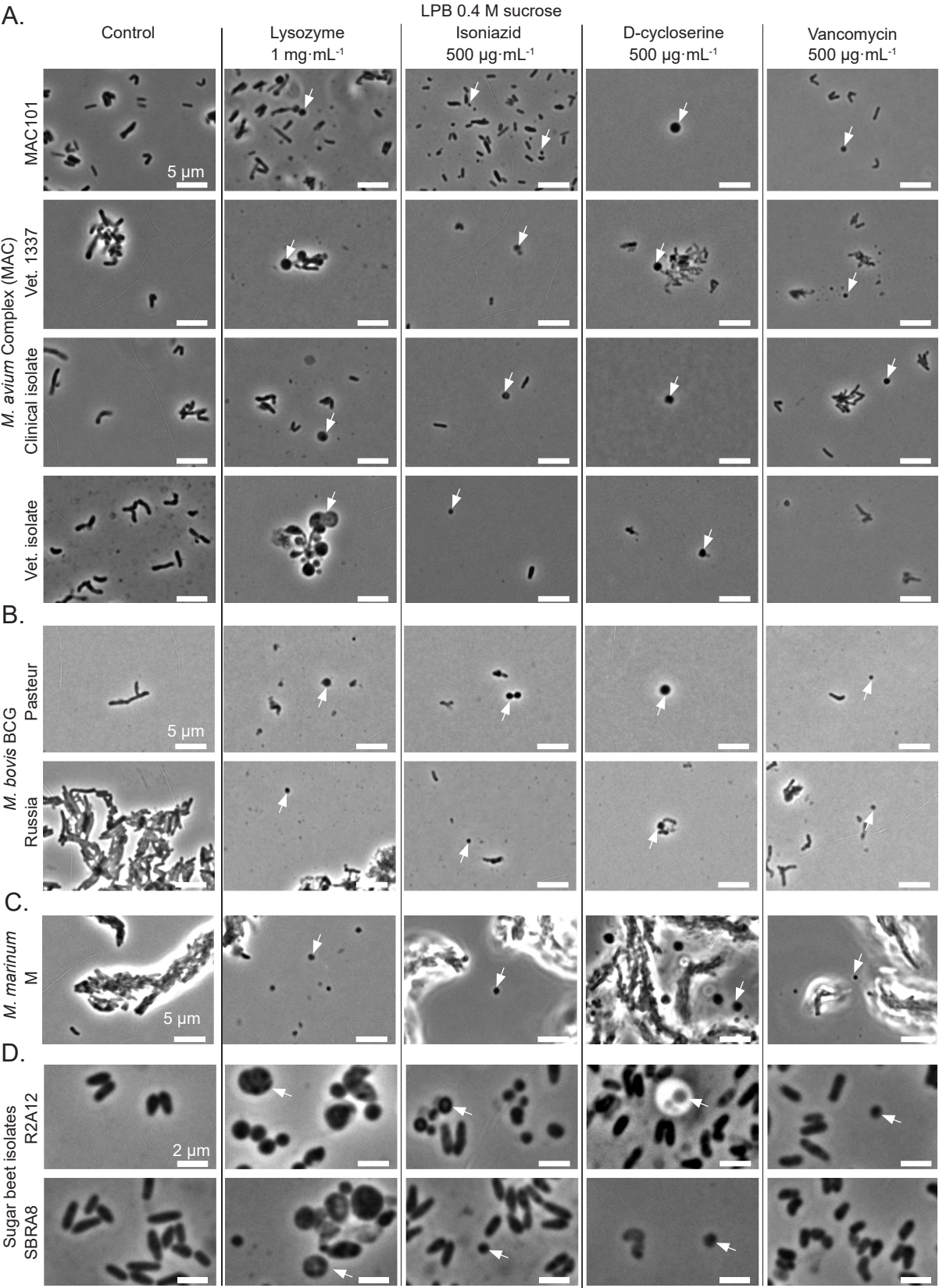C. *M. marinum* M

D. Sugar beet isolates: R2A12, SBRA8

Figure S9. Cell wall-targeting antibiotics induces the formation of CWD cells mycobacterial species

Phase-contrast images of various mycobacterial strains, namely **A)** *M. avium* Complex (MAC) strains. **B)** *M. bovis* BCG strains. **C)** *M. marinum* M strain and **D)** Endophyte sugar beet isolates, grown in LPB (0.4 M sucrose) supplemented with 500 µg·mL^{-1} of either isoniazid, D-cycloserine or vancomycin. Controls includes 1 mg·mL^{-1} Lysozyme + 25 mM MgCl2 (positive control) and no supplementation (negative Control). Scale bars represent either 5 or 2 µm.
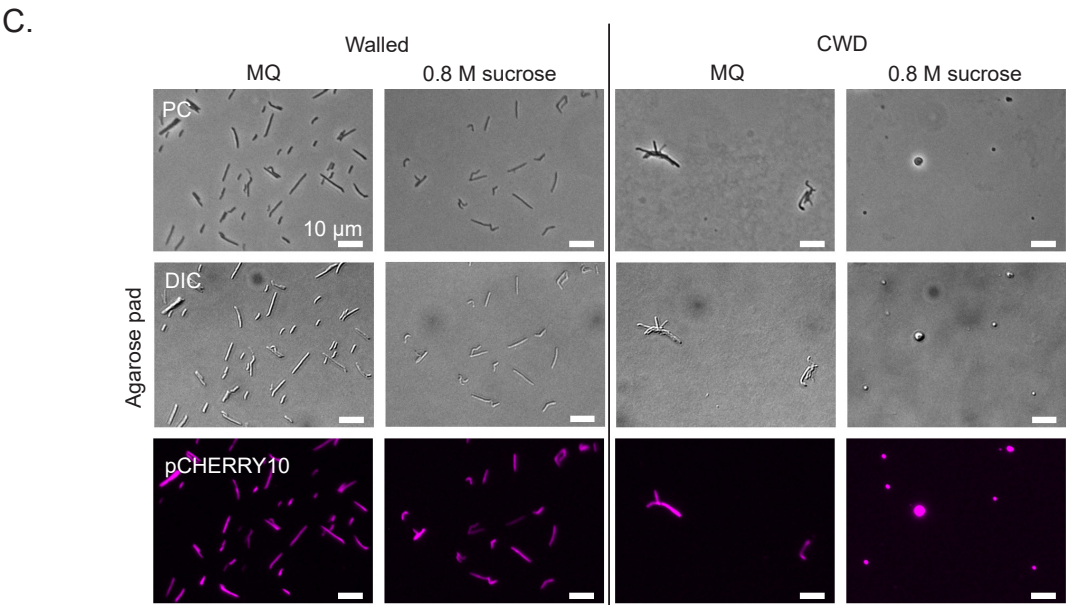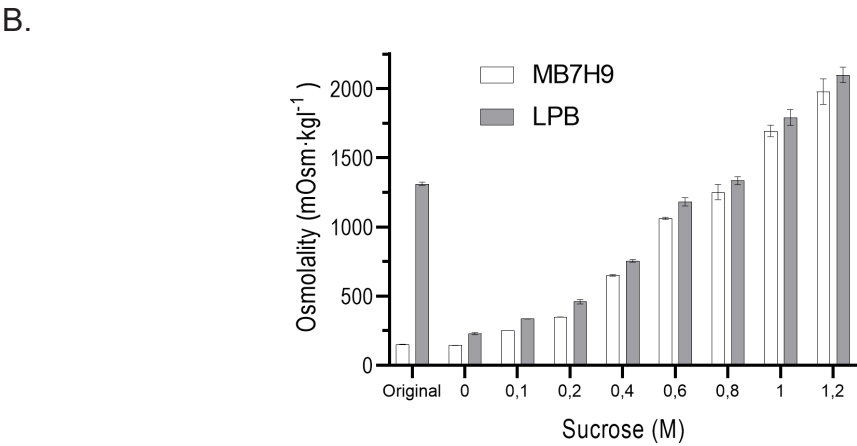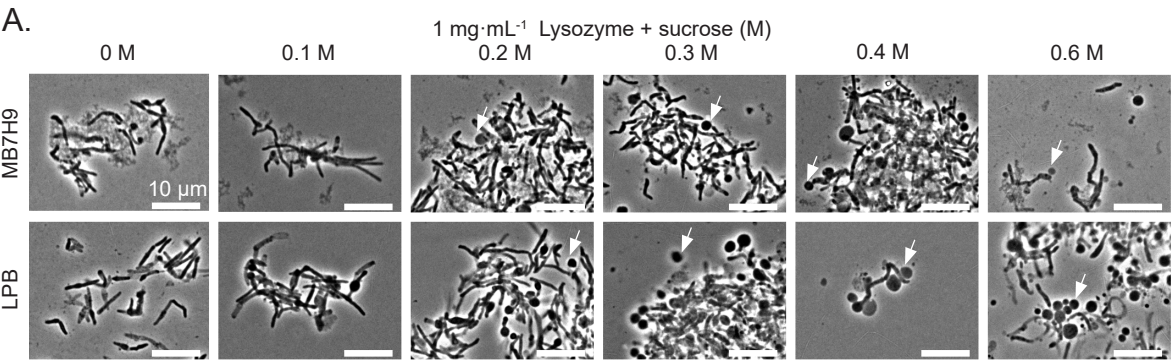
SUPPLEMENTAL FIGURE 10

A.

1 mg·mL^{-1} Lysozyme + sucrose (M)

0 M 0.1 M 0.2 M 0.3 M 0.4 M 0.6 M

MB7H9

LPB

10 µm

B.

C.

Walled — MQ, 0.8 M sucrose

CWD — MQ, 0.8 M sucrose

PC

DIC

pCHERRY10

Agarose pad

10 µm

Figure S10. Mycobacterial CWD cells require osmolytes
A) Phase contrast images of M. smegmatis mc2155 exposed to 1 mg·mL-1 Lysozyme + 25 mM MgCl2 for 24 hours in either MB7H9 or LPB supplemented with ascending concentrations of sucrose. Scale bars represent 10 μm. **B)** Osmolality measurements of LPB and MB7H9 with ascending concentrations of sucrose. Original media includes standard used LPB at RT and MB7H9 kept at 4 °C. Measurements were performed in sextuplicate. **C)** Phase contrast, DIC and fluorescent micrographs of M. smegmatis mc2155::pCHERRY10 walled grown in MB7H9 and CWD cells enriched from LPB (1.0 M sucrose) mounted on MQ and MQ/sucrose (0.8 M sucrose) agar pads. Please note that all CWD cells are absent when placed on MQ agar pads. Scale bars represent 10 μm.